①

SCATTERING FROM A PLANAR
EQUIANGULAR SPIRAL ANTENNA

THESIS
Stephen C. Moraites
Captain, USAF

AFIT/GE/ENG/85D-27

DTIC
ELECTE
MAY 12 1986
S   D
B

DEPARTMENT OF THE AIR FORCE
AIR UNIVERSITY

AIR FORCE INSTITUTE OF TECHNOLOGY

Wright-Patterson Air Force Base, Ohio

86 5   12 027

SCATTERING FROM A PLANAR
EQUIANGULAR SPIRAL ANTENNA

THESIS
Stephen C. Moraites
Captain, USAF

AFIT/GE/ENG/85D-27

DTIC
ELECTE
MAY 1 2 1986
S   D
B

AFIT/GE/ENG/85D-27

SCATTERING FROM A PLANAR EQUIANGULAR SPIRAL ANTENNA

THESIS

Presented to the Faculty of the School of Engineering

of the Air Force Institute of Technology

Air University

In Partial Fulfullment of the

Requirements for the Degree of

Master of Science in Electrical Engineering

Stephen C. Moraites, B.S.

Captain, USAF

December 1985

Preface

In this thesis, techniques are presented which will aid in the study of scattering from a loaded four arm planar equiangular spiral antenna. Extensive use was made of the references listed in the bibliography and the serious reader is encouraged to study those references. By understanding the content of the references, and therefore the structure on which this thesis is built, the reader should be able to extend the techniques described here to other equiangular spiral antennas and possibly to other frequency independent antennas.

I would like to acknowledge my thesis advisor, Dr. A. J. Terzuoli for extending to me the flexibility required in this creative effort. I wish also to thank my wife, Kelly, for her multifaceted support.
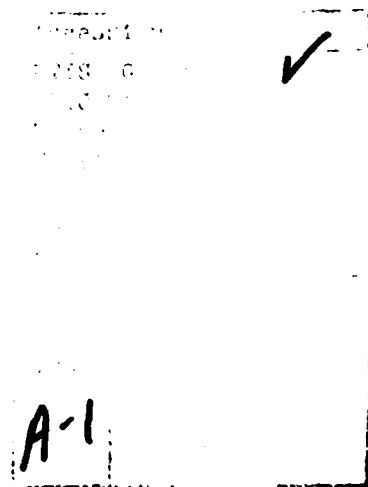
Stephen Charles Moraites

A-1

ii

Table of Contents

List of Figures

Abstract

This thesis presents analytical and numerical techniques for analyzing the scattering from a planar equiangular spiral antenna loaded at its terminals. The scattering matrix for the loaded antenna is derived as a function of the antenna load impedance. This derivation is the result of an analytical study of the voltage/current relationship at the antenna terminals along with an application of a multiport analysis of the scattering problem. A numerical technique is also developed that utilizes at different wavelengths common elements of the generalized impedance matrix of the moment method solution. This technique provides for rapid computation of the scattering properties of the spiral antenna across a band of frequencies.

CHAPTER 1

Introduction

This thesis pertains to the electromagnetic scattering properties of a loaded four arm planar equiangular spiral antenna.

The spiral antenna is one of a class of antennas with frequency independent properties (17). As a radiating device, its properties have been measured (4), analyzed (17), and exploited (9;21). As a scatterer however, no published work has yet fully characterized this structure. This thesis addresses two questions on the problem of determining the scattering properties of the loaded four arm planar equiangular spiral:

1. What effect does the antenna load have on the scattering properties?

2. How can the special geometry of the symmetric, self complementary, equiangular spiral be used in the numerical analysis of this scatterer?

These two questions will be dealt with, respectively, in this thesis by accomplishing the following:

1. An expression is derived which gives the scattering matrix of the antenna as a function of antenna load impedance. The expression is in terms of theoretically determined parameters and numerically determined parameters (from the method of moments.)

2. Techniques are developed that decrease the computation time of the numerically determined parameters. These techniques are developed from the special geometric properties of the antenna.

1

The importance of antenna scattering theory lies in its applicability to remote prediction of antenna parameters, field measurements, radar cross section studies, and electromagnetic compatibility. Previous work pertaining to antenna scattering is readily found in the literature. Various approaches to studying antenna scattering are

1. spherical mode expansion of the incident field (3:317-329)

2. multiport systems analysis (6:107-125)

3. equivalent circuit analysis (5:1-23)

4. receiver antenna current analysis (5:1-23)

5. numerical computation; e.g. moment method solution of the field equations (6)

Green's work (5) provides a survey of approaches 1 through 5 and is a standard reference on the subject.

This thesis approaches the problem of antenna scattering by describing the scattering situation as a multiport system whose parameters are found both analytically and through numerical computation. A complete analysis of the multiport requires a knowledge of the port parameters that relate the port currents to the port voltages. Chapter 2 of this thesis presents the derivation of the port parameters for the four arm planar equiangular spiral antenna. Also within Chapter 2 is information on the radiation properties of the antenna that is pertinent to the subsequent scattering analysis.

Chapter 3 formulates the problem of scattering by a loaded four arm spiral. Here the measurement port is added to the multiport system and the relationship among the various port

parameters is explained. The end result of Chapter 3 is an expression for the scattering matrix as a function of the scattering antenna load impedance. This expression is in terms of scattering matrices of the antenna with its terminals shorted in various ways. Each of these "shorted" scattering matrices can be computed numerically using the method of moments.

Chapter 4 briefly explains the moment method as applied to the spiral antenna. Techniques are developed that exploit the very special geometry of the planar equiangular spiral and allow one to compute the scattering properties of the antenna over a band of frequencies with a minimum of computation time.

Chapter 5 is the conclusion and includes suggestions on the implementation of the analytical tools provided by this thesis.

CHAPTER 2

The Spiral Antenna

Geometry

A four arm planar equiangular spiral antenna is drawn in Figure 2.1. The spirals forming the edges of the arms are described by the polar equation 2.1 (4:182; 17:14)

$$\Theta=\Theta_0+[\tan(A)]\ln\rho \qquad (2.1)$$

or

$$\rho=a \exp[\alpha(\Theta-\delta)] \qquad (2.2)$$

where ρ and Θ are standard polar coordinates and the remaining constants are parameters that determine the expansion rate and angular position of the spiral. From the form of equation (2.1), it is apparent that two angles, Θ_0 and A completely define the geometry of an infinite spiral. The performance of an antenna whose geometry is entirely determined by angles is independent of frequency (17:13). If the arms of an infinite spiral antenna are truncated so as to be physically realizable, the spiral structure still performs -- in an antenna sense -- as the infinite structure does, provided that the frequency of operation remains within certain bounds.
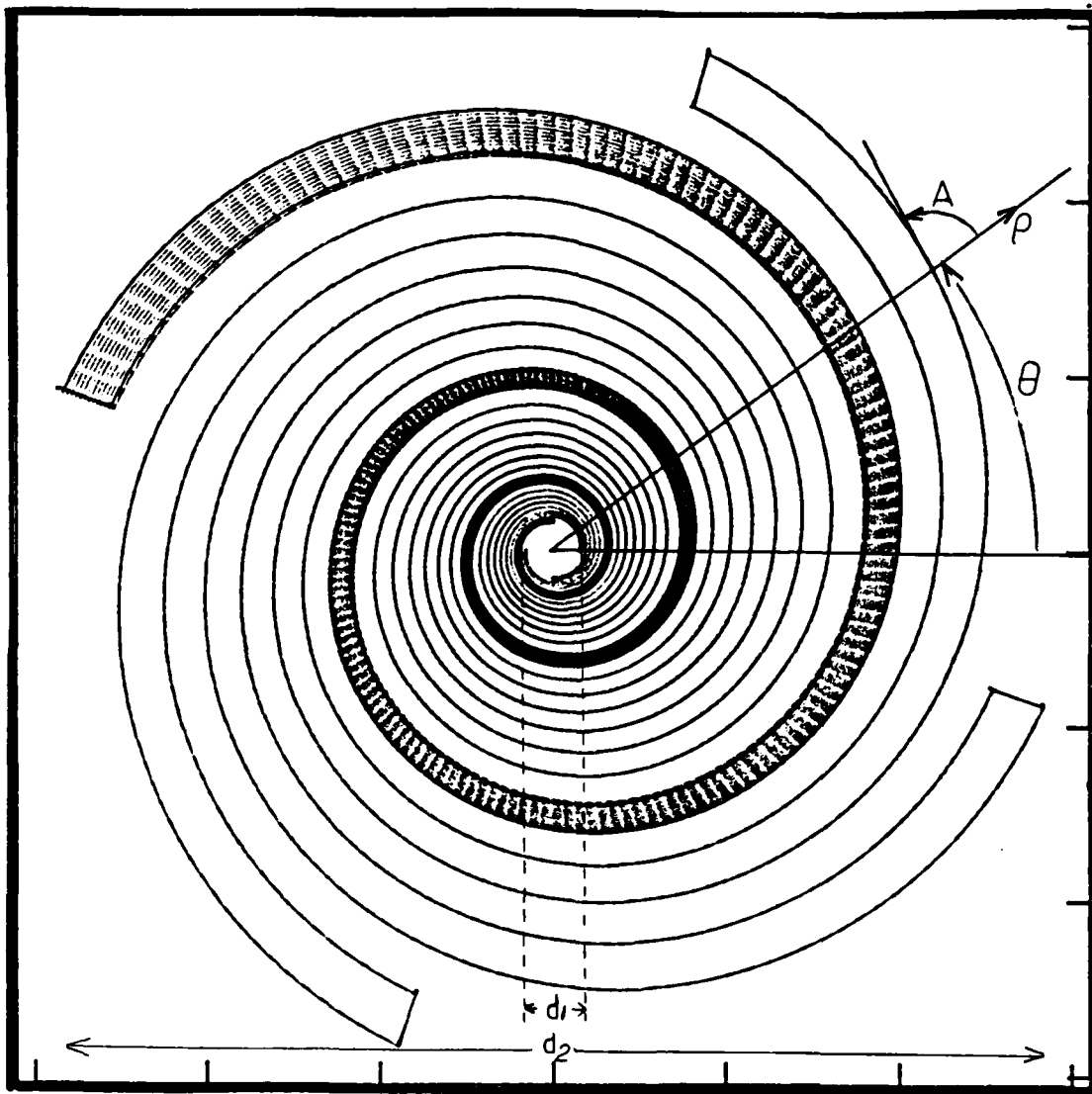
Figure 2.1. Four Arm Planar Equiangular Spiral Geometry.
Source: (17:14)

Bandwidth

Frequency independent performance of the infinite spiral antenna means 1) the antenna terminal impedances are independent of frequency; and 2) the radiation pattern is independent of frequency (17:13). Over the bandwidth of the truncated spiral antenna, the antenna's impedance and pattern will be treated as independent of frequency. Using the frequency bounds stated by Mosko (9:98), the upper limit is given by $\lambda_u = \pi d_1$ and the lower limit by $\lambda_L = \pi d_2/3$ where d_1 and d_2 are as shown in Figure 2.1. (These bounds permit multimode operation). Thus the antenna shown in Figure 2.1 has a 6 to 1 frequency range.

Terminal Impedances

Before considering terminal impedances of a four terminal spiral antenna, one should be familiar with the impedance relationship of single port planar complementary antennas. (Planar complementary antennas are a pair of structures that when superimposed, one on the other, exactly fill a plane with no overlap.) Given two such antennas:

$$ZZ_c = \eta_0^2/4 \approx (60\pi)^2 \qquad (2.3)$$

where Z and Z_c are the input impedances of an antenna and its complement (2:S371), and η_0 is the characteristic impedance of free space. If an antenna is its own complement, then $Z = Z_c \approx 60\pi$. Deschamps extended this relationship to multi-terminal, self complementary structures (2). Referring to

6

Figure 2.2, which shows the voltage and current conventions for a four terminal spiral antenna, the relationship between voltages and currents is, from Deschamps,

$$
\begin{bmatrix} \upsilon_0 \\ \upsilon_1 \\ \upsilon_2 \\ \upsilon_3 \end{bmatrix} = \begin{bmatrix} \zeta_0 & \zeta_1 & \zeta_2 & \zeta_3 \\ \zeta_3 & \zeta_0 & \zeta_1 & \zeta_2 \\ \zeta_2 & \zeta_3 & \zeta_0 & \zeta_1 \\ \zeta_1 & \zeta_2 & \zeta_3 & \zeta_0 \end{bmatrix} \begin{bmatrix} i_0 \\ i_1 \\ i_2 \\ i_3 \end{bmatrix}
\tag{2.4}
$$

or

$$
[\upsilon] = [\zeta][i]
\tag{2.5}
$$

Application of Deschamps' work to a four arm planar equiangular spiral antenna requires evaluation of the following transformation:

$$
\begin{bmatrix} \zeta_0 \\ \zeta_1 \\ \zeta_2 \\ \zeta_3 \end{bmatrix} = \begin{bmatrix} 1 & 1 & 1 & 1 \\ 1 & -j & -1 & j \\ 1 & -1 & 1 & -1 \\ 1 & j & -1 & -j \end{bmatrix} \begin{bmatrix} \xi_0 \\ \xi_1 \\ \xi_2 \\ \xi_3 \end{bmatrix} \frac{1}{4}
\tag{2.6}
$$

where

$$
\xi_m = \eta_0/4\sin(m\pi/4) \qquad m=1,2,3
$$
$$
\xi_0 = 0
$$

The reader should refer to reference 2 for details of the derivation of equations (2.4) and (2.6). The evaluation of equation 2.6 yields

$$
\begin{bmatrix} \zeta_0 \\ \zeta_1 \\ \zeta_2 \\ \zeta_3 \end{bmatrix} = \frac{\eta_0}{16} \begin{bmatrix} 1+2\sqrt{2} \\ -1 \\ 1-2\sqrt{2} \\ -1 \end{bmatrix}
\tag{2.7}
$$

7

$$\sum_{i=0}^{3} \upsilon_i = 0$$

$$\sum_{i=0}^{3} i_i = 0$$
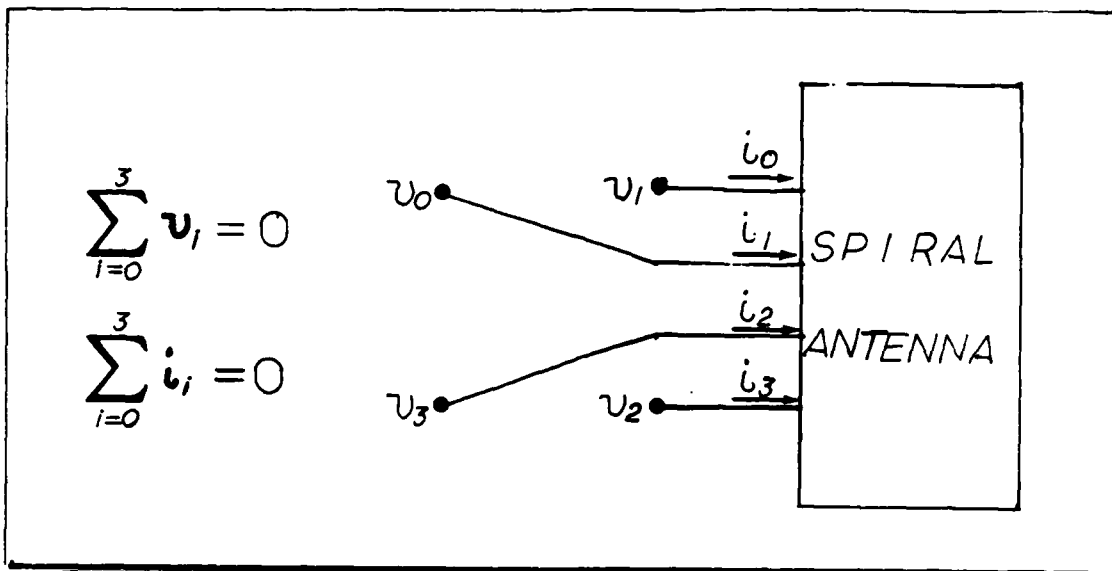
Figure 2.2. Terminal Voltage and Terminal Current Convention

From a mathmatical point of view, the system of equations 2.4 has meaning only on a hyperplane imbedded in four-space. In the derivation of equation 2.4, the requirement was made that $\sum \upsilon_i = 0$ and $\sum i_i = 0$. Therefore, there are only three independent coordinates of the vector space spanned by $[\upsilon]$ or $[i]$. It will prove useful to apply a transformation of coordinates that allows one to arbitrarily fix the value of one transformed component of $[i]$ to some convenient value. The transformation is a simple rotation in four-space about the origin. Its physical interpretation is shown in Figure 2.3. The four terminal currents are represented by the vector $[i]$. Now define branch currents [I] such that

$$\begin{bmatrix} i_0 \\ i_1 \\ i_2 \\ i_3 \end{bmatrix} = \begin{bmatrix} 1 & 0 & 0 & -1 \\ -1 & 1 & 0 & 0 \\ 0 & -1 & 1 & 0 \\ 0 & 0 & -1 & 1 \end{bmatrix} \begin{bmatrix} I_0 \\ I_1 \\ I_2 \\ I_3 \end{bmatrix} \tag{2.8}$$

8
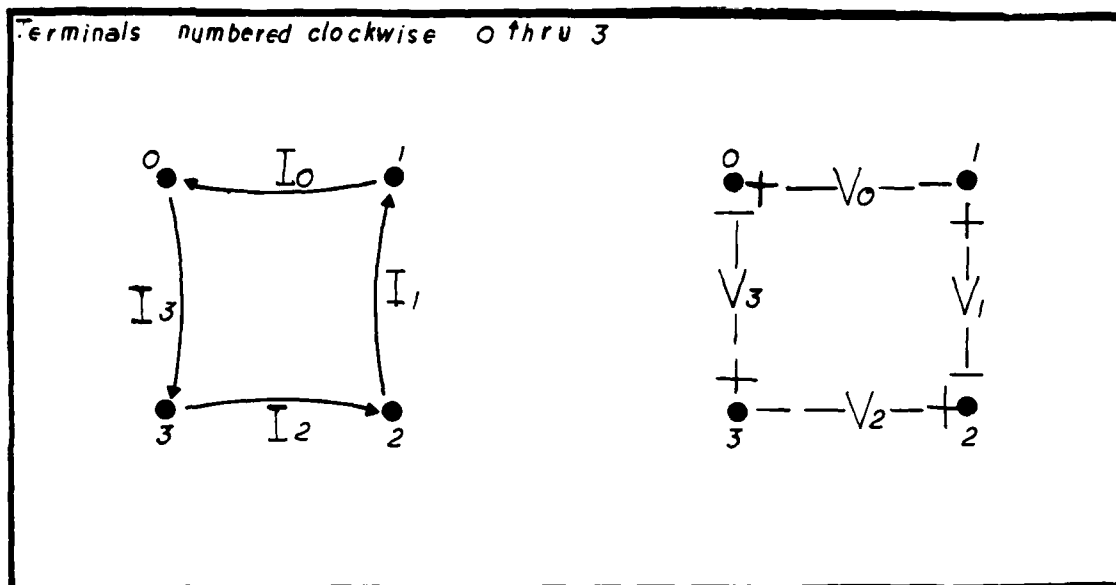
Figure 2.3.   Branch Current and Branch Voltage Conventions.

or

$$[i]=[T][I] \qquad (2.9)$$

And since the matrix relating $[i]$ to $[I]$ is of rank three, the complete solution for $[I]$ can be expressed as (9:211,219)

$$\begin{bmatrix} I_0 \\ I_1 \\ I_2 \\ I_3 \end{bmatrix} = t \begin{bmatrix} 1 \\ 1 \\ 1 \\ 1 \end{bmatrix} + \begin{bmatrix} i_0 \\ i_0 + i_1 \\ i_0 + i_1 + i_2 \\ 0 \end{bmatrix} \qquad (2.10)$$

which shows that $[I_3]$ may be arbitrarily fixed.

To simplify the subsequent analysis, the voltage vector $[v]$ will be transformed also. A new vector as shown in Figure 2.3 is defined by

9

$$
\begin{bmatrix} V_0 \\ V_1 \\ V_2 \\ V_3 \end{bmatrix} = \begin{bmatrix} 1 & -1 & 0 & 0 \\ 0 & 1 & -1 & 0 \\ 0 & 0 & 1 & -1 \\ -1 & 0 & 0 & 1 \end{bmatrix} \begin{bmatrix} \upsilon_0 \\ \upsilon_1 \\ \upsilon_2 \\ \upsilon_3 \end{bmatrix}
\tag{2.11}
$$

or

$$
[V] = [T]^T[\upsilon]
\tag{2.12}
$$

Equations (2.5), (2.9) and (2.12) can be rewritten as

$$
[V] = [Z][I]
\tag{2.13}
$$

where

$$
[Z] = [T]^T[\zeta][T]
$$

Evaluating [Z]:

$$
[Z] = \begin{bmatrix} Z_0 & Z_1 & Z_2 & Z_3 \\ Z_3 & Z_0 & Z_1 & Z_2 \\ Z_2 & Z_3 & Z_0 & Z_1 \\ Z_1 & Z_2 & Z_3 & Z_0 \end{bmatrix}
\tag{2.15}
$$

where

$$
\begin{bmatrix} Z_0 \\ Z_1 \\ Z_2 \\ Z_3 \end{bmatrix} = \begin{bmatrix} 2\zeta_0 - \zeta_1 - \zeta_3 \\ 2\zeta_1 - \zeta_2 - \zeta_0 \\ 2\zeta_2 - \zeta_3 - \zeta_1 \\ 2\zeta_3 - \zeta_0 - \zeta_2 \end{bmatrix} = \frac{\eta_0}{4} \begin{bmatrix} 1 + \sqrt{2} \\ -1 \\ 1 - \sqrt{2} \\ -1 \end{bmatrix}
\tag{2.16}
$$

The physical system described by equation 2.13 is shown in Figure 2.3.

Radiation Modes

By proper phasing of the terminal currents, $[i]$, one can obtain radiation patterns that are suitable for direction finding systems (9). Selection of three orthogonal phase schemes for the terminal currents leads to three independent modes of radiation. Two of the modes are shown in Figure 2.4.
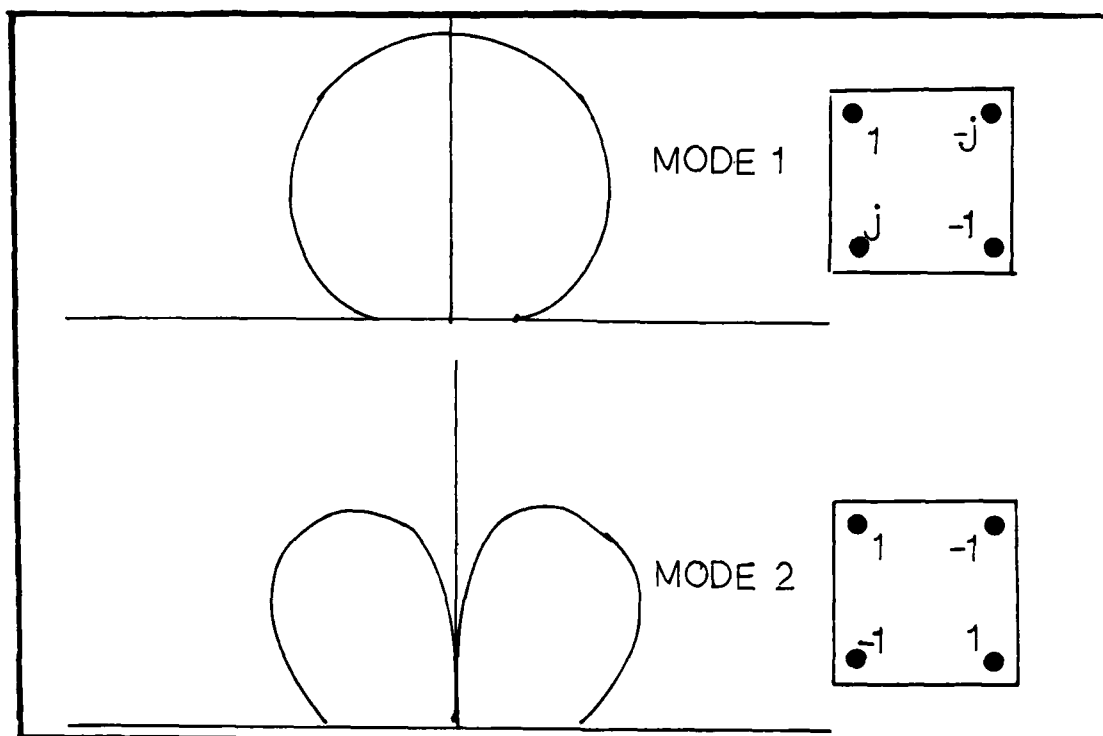
Figure 2.4. Radiation Patterns of Four Arm Spiral in Plane Perpendicular to Plane of Antenna. Phase of Terminal Currents Shown to Right of Patterns.

Source: (9;92)

Feed Point Configuration

To obtain the two modes shown in Figure 2.4, one must choose a method of feeding the antenna. Either mode could be created by feeding the structure with two balanced transmission lines. Figure 2.5 shows a feed method for either mode. This method, however, cannot be used if both modes are simultaneously required. If both modes are required, than the feed method shown in Figure 2.6 can be used. Physically, this method can be realized by running a coax cable to each terminal and connecting the outer conductors together. The impedance, Z, in the figures represents the internal impedance of the source as seen from the antenna.

11
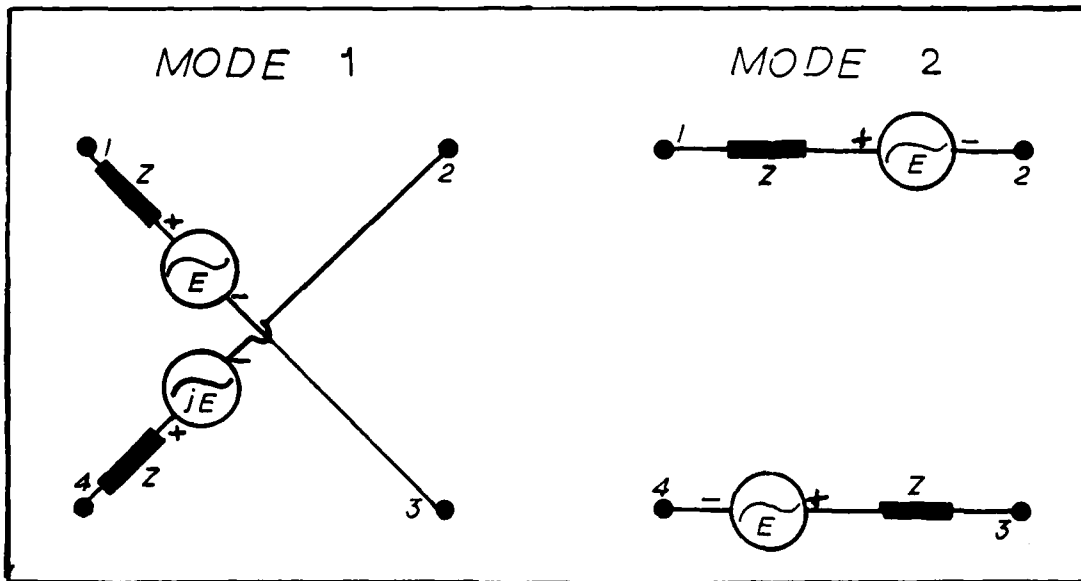
Figure 2.5.   Antenna Feed Networks for Single Mode
               Operation.
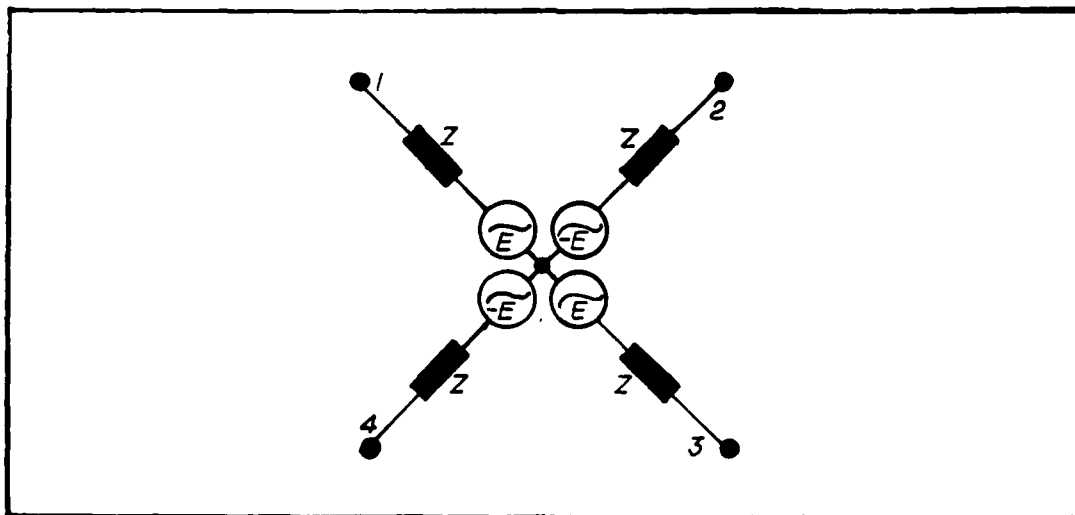
Figure 2.6.   Antenna Feed Network for Multi-mode
               Operation. Mode 2 Shown. Other Modes are
               Created by Changing Generator Phases.

When receiving energy from space, the antenna also sees an impedance, Z, caused by the receiver input impedance and the transmission line between the receiver and the antenna. Throughout this thesis, the impedance seen at the antenna by looking back through the transmission line and into any receiver circuitry is called the antenna load impedance. Chapter 3 is devoted to the effect of this load impedance on the antenna's scattering properties. The input impedance for a multiterminal antenna depends on the mode being radiated (9:100). From reference 9, or by use of equation 2.4, mode 1 antenna impedance is 133 ohms. Mode 2 antenna impedance is 94 ohms. This is the impedance seen by each generator (and generator impedance) in Figure 2.6.

Radiation Pattern

In free space, a planar spiral antenna radiates on both sides of the plane of the antenna. This thesis, however, deals with an antenna mounted on the surface of an absorbing cavity. Such antennas are constructed to eliminate reflections from structures behind the antenna. The polarization is elliptic such that the electric vector rotates as the spiral expands (17:40).

CHAPTER 3

The Loaded Spiral Scatterer

The theory of scattering from a loaded four arm equi-angular spiral antenna will be developed from more general cases of electromagnetic scattering. The formulation of the theory follows Harrington (8) but is modified so as to pertain to backscattering only.

Scattering, No Load

Consider a measurement antenna and the environment around it as a single port network shown in Figure 3.1. By removing any scatterer of interest from the environment and relating V_r to I_r, a specific ratio, Z_{rr} is obtained. Under scatterless conditions:

$$V_r^0 / I_r = Z_{rr}^0 \tag{3.1}$$

Where the superscript indicates no scatterer of interest is present.
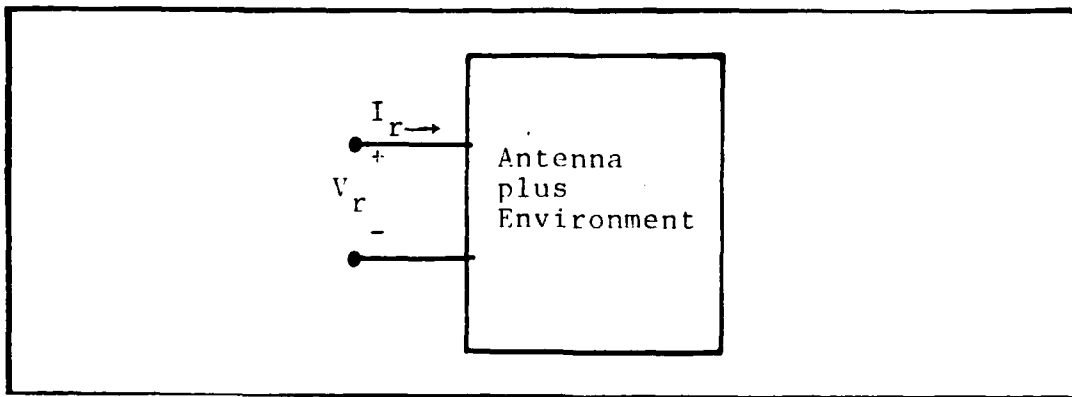
Figure 3.1. Single Port Representation of Scattering Situation.

14

Z_{rr}^{0} is the input impedance of the measurement antenna. Now if a scatterer is placed in the environment, the voltage V_r^s and the current I_r are related by

$$V_r^s / I_r = Z_{rr}^s \qquad (3.2)$$

Within the network of Figure 3.1, a wave is radiated from the measurement antenna, impinges on the scatterer and is scattered, with some of the scattered energy appearing as a voltage, ΔV_r, at the terminals of the measurement antenna:

$$\Delta V_r = V_r^s - V_r^0 \qquad (3.3)$$

A measure of the scatterer's effectiveness in reflecting energy back to its source is ΔZ_r, the scattering impedance.

$$\Delta Z_r = \Delta V_r / I_r \qquad (3.4)$$

The familiar measure, radar cross section, σ, is related to ΔZ_r as follows (7:167)

$$\sigma = 4\pi \left| \frac{2\lambda R^2}{\eta_0 \ell^2} \Delta Z_r \right|^2 \qquad (3.5)$$

where

    R = distance from scatterer to measurement antenna
    η_0 = characteristic impedance of free space
    ℓ = effective length of measurement antenna
    λ = wavelength of incident energy

In the analysis to follow, σ is an inadequate measure of the scatterer since phase information is lost in its definition. Note that the development so far also assumes some fixed

15

polarization for both the incident and scattered energy, the two being not necessarily the same. A more complete description of the scatterer is a scattering matrix (8:619) which relates the incident field E^i to the scattered field E^s:

$$\begin{bmatrix} E_1^S R \ \exp(jkr) \\ E_2^S R \ \exp(jkr) \end{bmatrix} = \begin{bmatrix} S_{11} & S_{12} \\ S_{21} & S_{22} \end{bmatrix} \begin{bmatrix} E_1^i \\ E_2^i \end{bmatrix} \tag{3.6}$$

where the subscripts refer to two orthogonal polarizations. S_{mn} and ΔZ_r are related by

$$S_{mn} = \frac{j2\lambda R^2}{\eta_0 \ell^2} \exp(2jkR) \ \Delta Z_r \tag{3.7}$$

Note that the dependence of ΔZ_r on m and n; that is, on the polarization of interest, is not explicit but is just as definite as in the S parameters.

Loaded Single Port Scattering

Now, returning to the network representation of the scattering problem, one can conceptualize the antenna scattering problem by adding an additional port to represent the terminals of the scatterer as in Figure 3.2.
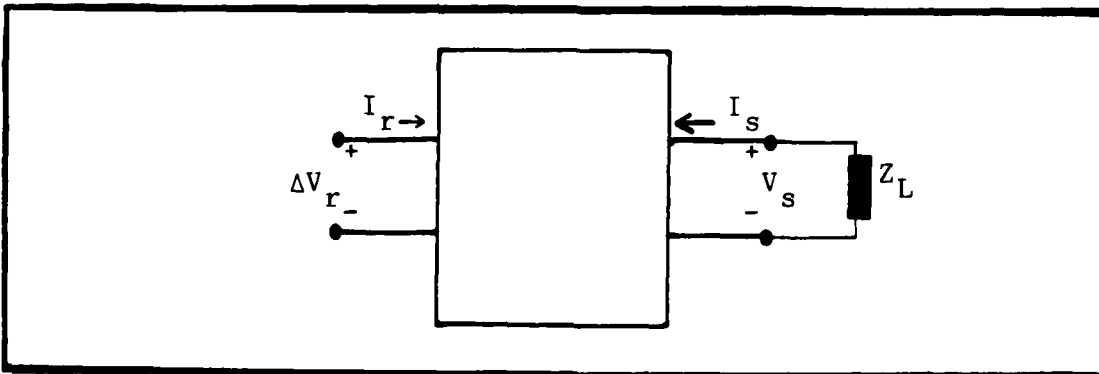
Figure 3.2. Single Port Scatterer Added to Network of Fig3.1

A matrix equation relating the port parameters is (7:166)

$$\begin{bmatrix} \Delta V_r \\ V_s \end{bmatrix} = \begin{bmatrix} \Delta Z_{rr} & Z_{rs} \\ Z_{sr} & Z_{ss} \end{bmatrix} \begin{bmatrix} I_r \\ I_s \end{bmatrix} \qquad (3.8)$$

where ΔV_r is defined in equation 3.3 and the Z variables are standard open circuit impedance parameters. If the scatterer is loaded with Z_L at its port, then $V_s = -Z_L I_s$ and equation 3.8 can be solved for the scattering impedance, $\Delta Z_r(Z_L)$:

$$\Delta Z_r(Z_L) = \frac{\Delta V_r}{I_r} = \left[\Delta Z_{rr} - \frac{Z_{rs} Z_{sr}}{Z_{ss} + Z_L} \right] \qquad (3.9)$$

Loaded Two Port Scattering

If the scatterer has two ports, the relationship among the port parameters is (8:618)

$$\begin{bmatrix} \Delta V_r \\ V_1 \\ V_2 \end{bmatrix} = \begin{bmatrix} \Delta Z_{rr} & Z_{r1} & Z_{r2} \\ Z_{1r} & Z_{11} & Z_{12} \\ Z_{2r} & Z_{21} & Z_{22} \end{bmatrix} \begin{bmatrix} I_r \\ I_1 \\ I_2 \end{bmatrix} \qquad (3.10)$$

or, making use of the load relations, $V_i = -Z_{Li} I_i$, and solving for the scattering impedance:

$$\Delta Z_r(Z_{L1}, Z_{L2}) = \frac{\Delta V_r}{I_r} = \left[\Delta Z_{rr} - \begin{bmatrix} Z_{r1} & Z_{r2} \end{bmatrix} \begin{bmatrix} Z_{11} + Z_{L1} & Z_{12} \\ Z_{21} & Z_{22} + Z_{L2} \end{bmatrix}^{-1} \begin{bmatrix} Z_{1r} \\ Z_{2r} \end{bmatrix} \right] \qquad (3.11)$$

where

$Z_{ri} = Z_{ir}$ = the open circuit impedance parameter between the measurement antenna and port i

Z_{ij} = open circuit impedance parameter between port i and j

Z_{Li} = load impedance at port i

$\Delta V_r = V_r^s - V_r^0$

17
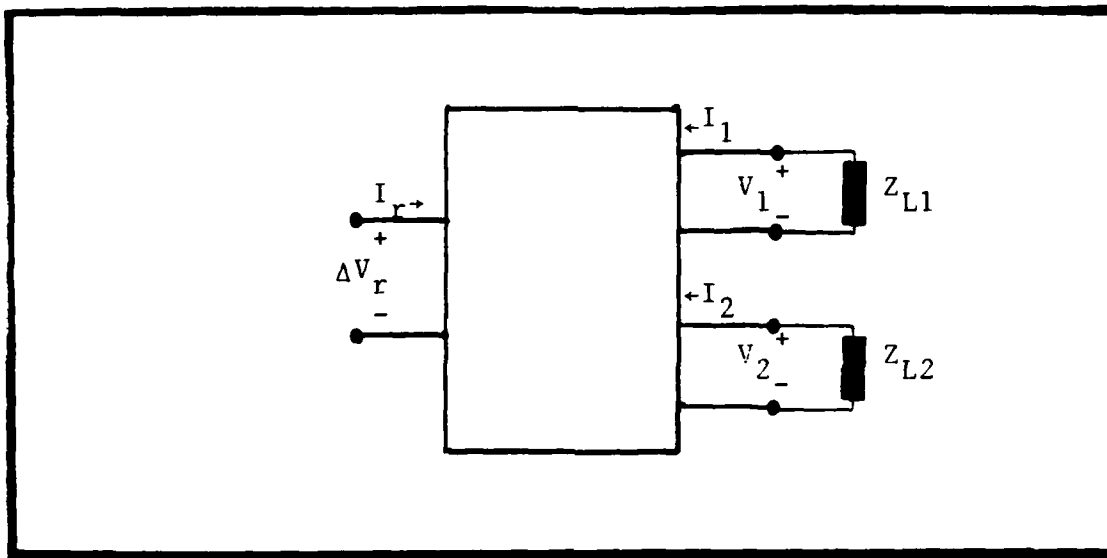
Figure 3.3. Network Representation of Scattering by a Two Port Scatterer Loaded with Z_{L1} and Z_{L2}.

Equations 3.10 and 3.11 can be used to represent the loaded four arm spiral antenna only if a definite terminal-to-port assignment is made and only if no self complementary two port theory (2:S377) is applied. (Because all the terminals meet at a point, the feed configuration at one port, however it's defined, will affect the feed configuration of the other port when the complement of the antenna is considered. The four terminal equiangular spiral is not a self complementary two port structure.)

Multiterminal Loaded Scattering

As explained in Chapter 2, a feed system more versatile than the two port may be required. The network representing the four terminal scattering system is shown in Figure 3.4.

18
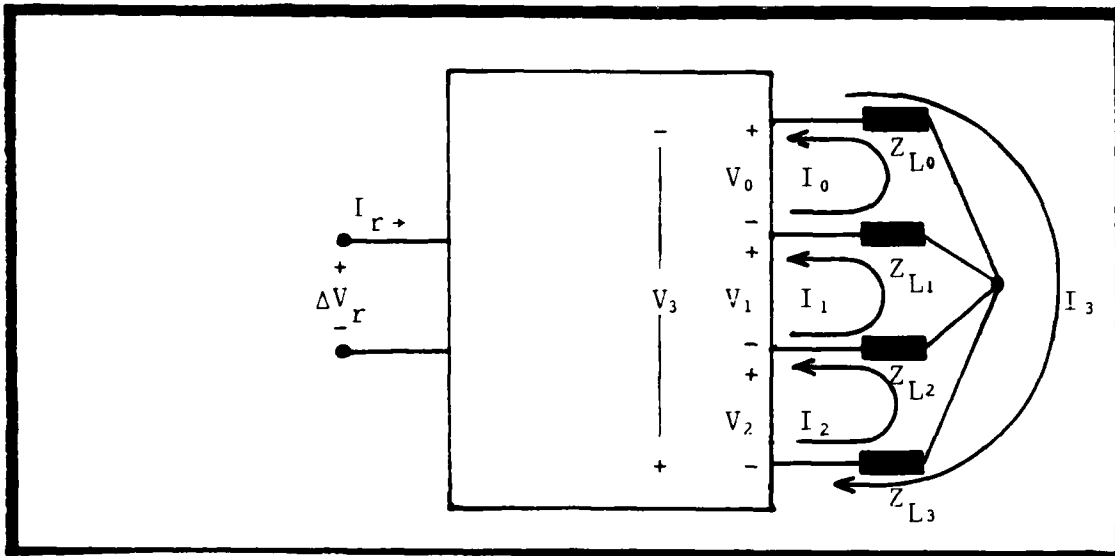
Figure 3.4. Network representation of Scattering by a Four Terminal Loaded Structure. (Measurement port on left)

Making use of equation 2.13, one can arrive at the system of equations describing Figure 3.4.

$$\begin{bmatrix} \Delta V_r \\ V_0 \\ V_1 \\ V_2 \\ V_3 \end{bmatrix} = \begin{bmatrix} \Delta Z_{rr} & Z_{r0} & Z_{r1} & Z_{r2} & Z_{r3} \\ Z_{0r} & Z_0 & Z_1 & Z_2 & Z_3 \\ Z_{1r} & Z_3 & Z_0 & Z_1 & Z_2 \\ Z_{2r} & Z_2 & Z_3 & Z_0 & Z_1 \\ Z_{3r} & Z_1 & Z_2 & Z_3 & Z_0 \end{bmatrix} \begin{bmatrix} I_r \\ I_0 \\ I_1 \\ I_2 \\ I_3 \end{bmatrix} \qquad (3.12)$$

or by separating the system and using the load constraints:

$$\Delta Z_r \begin{pmatrix} Z_{L0} \\ Z_{L1} \\ Z_{L2} \\ Z_{L3} \end{pmatrix} = \frac{\Delta V_r}{I_r} = \Delta Z_{rr} + \frac{\sum_0^3 Z_{rj} I_j}{I_r} \qquad (3.13)$$

and

$$-I_r \begin{bmatrix} Z_{0r} \\ Z_{1r} \\ Z_{2r} \\ Z_{3r} \end{bmatrix} = \begin{bmatrix} Z_0+Z_{L1}+Z_{L0} & Z_1-Z_{L1} & Z_2 & Z_3-Z_{L0} \\ Z_3-Z_{L1} & Z_0+Z_{L2}+Z_{L1} & Z_1-Z_{L2} & Z_2 \\ Z_2 & Z_3-Z_{L2} & Z_0+Z_{L3}+Z_{L2} & Z_1-Z_{L3} \\ Z_1-Z_{L0} & Z_2 & Z_3-Z_{L3} & Z_0+Z_{L0}+Z_{L3} \end{bmatrix} \begin{bmatrix} I_0 \\ I_1 \\ I_2 \\ I_3 \end{bmatrix}$$

Parameter Study

Before proceeding further to express equations 3.13 and 3.14 into more practical forms, one can gain insight into antenna scattering by considering the meaning of the various terms in the preceeding equations. With reference to equation 3.8, the parameter Z_{rs} is related to the scattering antenna power gain G (8:620):

$$G = C |Z_{rs}|^2 \qquad (3.15)$$

where the constant of proportionality includes measurement antenna parameters, distance, etc. so that G is a characteristic only of the scattering antenna's radiation properties. Another parameter, ΔZ_{rr} is the value of ΔZ_r when $Z_L = \infty$.

$$\Delta Z_{rr} = \Delta Z_r(\infty) \qquad (3.16)$$

In the analysis to follow, Z_{rs} and its multiport counterparts are unknown quantities and it is convenient to omit them from the equation. (Using the method of moments, described in Chapter 4, calculation of Z_{rs} requires the introduction of generators and wires in the antenna model. This addition is undesirable.) Solving for Z_{rs} in terms of open and short circuited scattering impedance yields

$$Z_{rs}^2 = Z_{ss}(\Delta Z_r(\infty) - \Delta Z_r(0)) \qquad (3.17)$$

Substitution and further manipulation lead to expressions similar to those derived by Green (5:24-26):

20

$$G = C \left| Z_r(\infty) - \Delta Z_r(0) \right|^2 \tag{3.18}$$

$$\Delta Z_r(Z_L) = \frac{Z_L \Delta Z_r(\infty) + Z_{ss}\Delta Z_r(0)}{Z_{ss} + Z_L} \tag{3.19}$$

$$\Delta Z_r(Z_L) = \Delta Z_r(Z_{ss}^*) + \frac{Z_{ss}[\Delta Z_r(\infty) - \Delta Z_r(0)](Z_L - Z_{ss}^*)}{(Z_{ss} + Z_{ss}^*)(Z_{ss} + Z_L)} \tag{3.20}$$

Equation 3.20 allows one to define a structural and antenna component of the scattered field. $\Delta Z_r(Z_{ss}^*)$ of the right hand side is termed the structural component and the remainder of the right hand side is termed the antenna component since it goes to zero when the antenna load impedance Z_L equals the conjugate of the antenna input impedance, Z_{ss}.

Referring now to equation 3.10 describing the two port representation, Z_{r1} and Z_{r2} are related to the radiation properties from their respective ports of the scattering antenna. When $I_r = 0$, the voltage at the measurement antenna is

$$V_r = I_1 Z_{r1} + I_2 Z_{r2} \tag{3.21}$$

so

$$G = C \left| I_1 Z_{r1} + I_2 Z_{r2} \right|^2 \tag{3.22}$$

Again, solving for Z_{ri} in terms of open and short circuited scattering impedances:

$$Z_{r2}^2 = Z_{22} \left[\Delta Z_r(\infty, \infty) - \Delta Z_r(\infty, 0) \right] \tag{3.23}$$

21

and

$$Z_{r1}^2 = Z_{11}\left[\Delta Z_r(\infty,\infty) - \Delta Z_r(0,\infty)\right] \qquad (3.24)$$

therefore

$$G = C\left\{\sqrt{Z_{11}\left[\Delta Z_r(\infty\infty) - \Delta Z_r(0,\infty)\right]}\,I_1 + \sqrt{Z_{22}\left[\Delta Z_r(\infty\infty) - \Delta Z_r(\infty,0)\right]}\,I_2\right\}^2 \qquad (3.25)$$

Further manipulation of the two port equations yields

$$\Delta Z_r(Z_{L1},Z_{L2}) =$$

$$\frac{Z_{L1}Z_{L2}\ Z(\infty,\infty) + Z_s Z_{L2}\Delta Z(0,\infty) + Z_s Z_{L1}\Delta Z(\infty,0) + (Z_s^2 - Z_x^2)\Delta Z(0,0)}{(Z_s + Z_{L1})(Z_s + Z_{L2}) - Z_x^2} \qquad (3.26)$$

where

$$Z_s = Z_{11} = Z_{22} \text{ of equation 3.10}$$
$$Z_x = Z_{12} = Z_{21} \text{ of equation 3.16}$$

Note the assumption that the ports are defined such that
$Z_{11} = Z_{22}$ and $Z_{12} = Z_{21}$. It can be shown from equation 2.13
that the two port impedances are real. Therefore, a conjugate
load impedance is real and equal to some Z_i. Thus

$$\Delta Z_r(Z_i,Z_i) = \frac{Z_s\left[\ Z(\infty,0) + \Delta Z(0,\infty)\right] + Z_i\left[\Delta Z(\infty,\infty) + Z(0,0)\right]}{2(Z_s + Z_i)} \qquad (3.27)$$

which is the structural component of the scattered field for
the particular terminal to port assignment. Note that, unlike
a single port scatterer, a two port scatterer does not have
a unique structural scattering component since the terminal
configuration and so the conjugate load, Z_i, can vary.

22

Referring finally to equations 3.13 and 3.14 describing
the more general loaded four terminal structure, the transfer
impedances Z_{ri} are analogous to their two port counterparts:

$$Z_{r_0}^2 = Z_0 \left[\Delta Z_r \begin{pmatrix} \infty \\ \infty \\ \infty \\ \infty \end{pmatrix} - \Delta Z_r \begin{pmatrix} 0 \\ 0 \\ \infty \\ \infty \end{pmatrix} \right] \qquad (3.28)$$

$$Z_{r_1}^2 = Z_0 \left[\Delta Z_r \begin{pmatrix} \infty \\ \infty \\ \infty \\ \infty \end{pmatrix} - \Delta Z_r \begin{pmatrix} \infty \\ 0 \\ 0 \\ \infty \end{pmatrix} \right] \qquad (3.29)$$

$$Z_{r_2}^2 = Z_0 \left[\Delta Z_r \begin{pmatrix} \infty \\ \infty \\ \infty \\ \infty \end{pmatrix} - \Delta Z_r \begin{pmatrix} \infty \\ \infty \\ 0 \\ 0 \end{pmatrix} \right] \qquad (3.30)$$

$$Z_{r_3}^2 = Z_0 \left[\Delta Z_r \begin{pmatrix} \infty \\ \infty \\ \infty \\ \infty \end{pmatrix} - \Delta Z_r \begin{pmatrix} 0 \\ \infty \\ \infty \\ 0 \end{pmatrix} \right] \qquad (3.31)$$

and

$$G = C \left| I_0 Z_{r_0} + I_1 Z_{r_1} + I_2 Z_{r_2} + I_3 Z_{r_3} \right|^2 \qquad (3.32)$$

In order to express equation 3.13 in terms not containing
Z_{ri}, one can make use of the results of Chapter 2 and let
$I_3 = 0$. Also, the last equation of the system of equations
3.14 can be dropped since $V_3 = -(V_0 + V_1 + V_2)$. Appendix A
contains the details of the algebra. The following results
apply to the case where $Z_{Li} = Z_L$ $i = 0, 1, 2, 3$ and use is made of
the equality between Z_1 and Z_3 of equation 3.12:

23

$$\Delta Z_r \begin{pmatrix} Z_L \\ Z_L \\ Z_L \\ Z_L \end{pmatrix} = \Delta Z_r \begin{pmatrix} \infty \\ \infty \\ \infty \\ \infty \end{pmatrix}$$

$$+F_1 \left[\Delta Z_r \begin{pmatrix} \infty \\ \infty \\ 0 \\ 0 \end{pmatrix} - \Delta Z_r \begin{pmatrix} \infty \\ \infty \\ \infty \\ \infty \end{pmatrix} \right]$$

$$+F_1 \left[\Delta Z_r \begin{pmatrix} 0 \\ \infty \\ \infty \\ 0 \end{pmatrix} - \Delta Z_r \begin{pmatrix} \infty \\ \infty \\ \infty \\ \infty \end{pmatrix} \right]$$

$$+F_1 \left[\Delta Z_r \begin{pmatrix} 0 \\ 0 \\ \infty \\ \infty \end{pmatrix} - \Delta Z_r \begin{pmatrix} \infty \\ \infty \\ \infty \\ \infty \end{pmatrix} \right]$$

$$+F_1 \left[\Delta Z_r \begin{pmatrix} \infty \\ 0 \\ 0 \\ \infty \end{pmatrix} - \Delta Z_r \begin{pmatrix} \infty \\ \infty \\ \infty \\ \infty \end{pmatrix} \right]$$

$$+F_2 \left[\Delta Z_r \begin{pmatrix} \infty \\ 0 \\ \infty \\ 0 \end{pmatrix} - \Delta Z_r \begin{pmatrix} \infty \\ \infty \\ \infty \\ \infty \end{pmatrix} \right]$$

$$+F_2 \left[\Delta Z_r \begin{pmatrix} 0 \\ \infty \\ 0 \\ \infty \end{pmatrix} - \Delta Z_r \begin{pmatrix} \infty \\ \infty \\ \infty \\ \infty \end{pmatrix} \right] \tag{3.33}$$

where

$$F_1 = Z_0(Z_L+(Z_0+Z_1))^2/D = Z_0/(Z_L+Z_1)$$
$$F_2 = 2(Z_0+Z_1)[(Z_L-Z_1)^2-Z_2^2]/D$$
$$D = [Z_L+(Z_0+Z_1)]^2[Z_L-Z_1]$$

Equation 3.33 expresses the scattering impedance, ΔZ_r, as a function of the antenna load impedance, Z_L. The expression is in terms of analytically determined parameters Z_i from equation 2.16 and numerically determined parameters $\Delta Z_r[\,]$. Since, as will be explained in Chapter 4, the scattering matrix of equation 3.6 is the representation of the scatterer most easily obtained, equation 3.33 can be rewritten in scattering matrix notation. From equation 3.7, each element of S is related to its corresponding ΔZ_r by the same factor.

As a result, the matrix S is a function of the antenna load impedance and is equal to

$$S\begin{pmatrix} Z_L \\ Z_L \\ Z_L \\ Z_L \end{pmatrix} = S\begin{pmatrix} \infty \\ \infty \\ \infty \end{pmatrix} + F_1\left\{\left[S\begin{pmatrix} \infty \\ 0 \\ \infty \end{pmatrix} - S\begin{pmatrix} \infty \\ \infty \\ \infty \end{pmatrix}\right] + \left[S\begin{pmatrix} 0 \\ \infty \\ 0 \end{pmatrix} - S\begin{pmatrix} \infty \\ \infty \\ \infty \end{pmatrix}\right] + \left[S\begin{pmatrix} 0 \\ \infty \\ \infty \end{pmatrix} - S\begin{pmatrix} \infty \\ 0 \\ \infty \end{pmatrix}\right]\right.$$

$$\left. + \left[S\begin{pmatrix} \infty \\ 0 \\ 0 \end{pmatrix} - S\begin{pmatrix} \infty \\ \infty \\ \infty \end{pmatrix}\right]\right\} + F_2\left\{\left[S\begin{pmatrix} \infty \\ 0 \\ 0 \end{pmatrix} - S\begin{pmatrix} \infty \\ \infty \\ \infty \end{pmatrix}\right] + \left[S\begin{pmatrix} \infty \\ \infty \\ \infty \end{pmatrix} - S\begin{pmatrix} \infty \\ \infty \\ \infty \end{pmatrix}\right]\right\} \qquad (3.34)$$

where F_1 and F_2 are as in equation 3.33.

Regarding the concept of structural and antenna components of the scattered field, each radiation mode will have its own input impedance (9:100) therefore, the proper conjugate matched load will depend on the mode under consideration. Since a single impedance value for Z_L cannot provide a match for all modes simultaneously, the concept of a structural component does not have the meaning it had for the single port.

CHAPTER 4

Field Computation

Formulation of the Problem

The end objective of the field computation at hand is to
have a numerical value for a complex matrix S (equation 3.6)
that expresses the magnitude and phase of the scattered
electric field at a point in space. The problem of obtaining
this end objective is divided into three subproblems:

1. Select the incident field
    a. wavelength
    b. polarization

2. Find the induced surface current on the scatterer

3. Compute the electric field due to the surface
    current

Then, by making use of equation 3.6, the scattering matrix,
S, can be computed. The numerical technique used to accomplish
the necessary computation is the moment method. Throughout
this thesis, Newman's Electromagnetic Surface Patch (ESP)
code (12) is the implementation of the moment method that is
used as a reference. If one makes use of this code directly,
then subproblem 1 is normally taken care of by the required
inputs to the code. The solutions to subproblems 2 and 3
and the computation of S are standard outputs. If one needs
to make use of the techniques explained in this chapter,
however, then some reorganization of this code is required.
For this reason, the three subproblems are identified and
explained seperately. Since the rational for choosing a

method of solving each subproblem is based on the subsequent step, the subproblems will be explained in reverse order.

Computation of the Fields

From field equivalence theorems (18:518,519), the electromagnetic field reflected from the surface, S, of a material body is equivalent to the field generated by appropriate surface currents on S in free space. In the case of a thin, flat, perfect conductor, the equivalent surface currents on the two flat sides may be considered equal and coincident. A single electric surface current on the open surface of a zero thickness plane can be used to find the reflected fields if the single current is the vector sum of the two surface currents of the flat plate (11:784). The electric field from a surface current $\overline{J}_s(\overline{r})$ is given by

$$\overline{E}(\overline{r}) = \iint_S \Gamma(\overline{r},\overline{r}')J_s(\overline{r}')ds' = L(\overline{J}_s(\overline{r}')) \qquad (4.1)$$

where

   Γ is the free space Green's function
   $\overline{r}$ is symbolic for the complete set of spatial coordinates
   L is a linear operator relating surface current to the
      electric field

$\overline{J}_s$ is assumed known as an expansion of subsectional basis functions (6:11):

$$\overline{J}_s = \sum_{i=1}^{M} I_i \overline{J}_i \qquad (4.2)$$

27

where each $\overline{J}_i$ is defined only over a small patch of the entire surface and I_i is the complex amplitude. If $\overline{J}_i$ is chosen as a sinusoidal spatial variation in the current density, then equation (4.1) is known in closed form (15;18:370,401). References 10 and 11 explain the use of patches of sinusoidal surface currents to model surfaces. The approach to finding the total scattered electric field by solving for fields of sinusoidal surface currents on small patches of the scatterer requires that the surface to be modeled be subdivided into patches. Appendix B explains how to subdivide the spiral antenna.

Given, then, the functional form of $\overline{J}_i$ and its amplitude, the fields from all surface patch currents are calculated using the appropriate formula as in equation (4.1). The total scattered field is just the vector sum of the fields generated by $I_i\overline{J}_i$ i=1 to M, where M is the number of surface patch currents.

Computation of Surface Currents

Reaction. The induced surface currents on a scatterer are found by solving an integral equation. In this thesis, the Electric Field Integral Equation (EFIE), is considered. The EFIE is a specific form of the Reaction Integral Equation (RIE) (12:6). The moment method computer code used as a reference (12) makes use of the RIE.

Reaction is a measure of the effect of one electromagnetic source upon another (16). In the special but pertinent case

28

of only electric surface currents existing on a scatterer,
the reaction between two sources "a" and "b" is

$$\langle \overline{J}_a, \overline{E}_b \rangle = \iint_a \overline{J}_a \cdot \overline{E}_b \, ds \qquad (4.3)$$

where $\overline{J}_a$ is the source (surface) current on "a" and $\overline{E}_b$ is
the field at "a" from a source at "b". Reaction is reciprocal
(16:1483):

$$\langle \overline{J}_a, \overline{E}_b \rangle = \langle \overline{J}_b, \overline{E}_a \rangle \qquad (4.4)$$

Moment Method. From Maxwell's equations, it is known that
the electric field tangential to a perfect conductor is zero.
Specifically, the tangential electric field on the surface
of a spiral antenna is zero. If the electric field around an
antenna is decomposed into an incident and scattered field;
that is, if

$$\overline{E} = \overline{E}^i + \overline{E}^s \qquad (4.5)$$

then the boundary conditions imply

$$\overline{E}_{tan} = \overline{E}^i_{tan} + \overline{E}^s_{tan} = 0 \qquad (4.6)$$

or

$$\overline{E}^s_{tan} = -\overline{E}^i_{tan} \qquad (4.7)$$

29

Consider $\overline{E}^s$ to be radiated from some unknown surface current on the antenna. Using the linear operator of equation (4.1):

$$L(\overline{J}_s) = \overline{E}^s \qquad (4.8)$$

Now applying equation 4.8 to equation 4.7:

$$[L(\overline{J}_s)]_{tan} = -\overline{E}^s_{tan} \qquad (4.9)$$

The method of moments converts equation 4.9 into a system of equations whose solution is an approximation to $\overline{J}_s$ (6).

Let the approximation to $\overline{J}_s$ be denoted by $\overline{J}_s^*$. As a measure of the correctness of $\overline{J}_s^*$, the reaction between $\overline{J}_s^*$ and a test source, $\overline{J}_t$, is forced to equal the reaction between the correct current, $\overline{J}_s$, and $\overline{J}_t$. That is, with the aid of equation (4.9),

$$\iint_t \overline{J}_t \cdot [L(\overline{J}_s^*)]_{tan} \, ds = -\iint_t \overline{J}_t \cdot \overline{E}^i_{tan} \, ds \qquad (4.10)$$

As explained in the beginning of this chapter by equation 4.2, $\overline{J}_s^*$ is expressed as a sum of subsectional basis functions:

$$\overline{J}_s^* = \sum_{i=1}^{M} I_i \overline{J}_i \qquad (4.11)$$

Substituting this into equation 4.10,

$$\sum_{i=1}^{M} I_i \iint_t \overline{J}_t \cdot L(\overline{J}_i) ds = -\iint_t \overline{J}_t \cdot \overline{E}^i ds \qquad (4.12)$$

30

where the "tangential" notation of equation 4.10 is dropped
since the dot product of the electric field with the test
current (which is defined to exist only on the surface of
the antenna) selects only the tangential component. Now M
linearly independent test sources, W_i i=1 to M can be defined
so that M linearly independent equations of the form of
equation 4.12 result. With the aid of the reaction notation,
this system is

$$\begin{bmatrix} \langle W_1,L(J_1)\rangle & \langle W_1,L(J_2)\rangle & \cdots & \langle W_1,L(J_M)\rangle \\ \langle W_2,L(J_1)\rangle & \langle W_2,L(J_2)\rangle & & \\ \vdots & & & \\ \langle W_M,L(J_1)\rangle & \cdots & & \langle W_M,L(J_M)\rangle \end{bmatrix} \begin{bmatrix} I_1 \\ I_2 \\ \\ I_M \end{bmatrix} = \begin{bmatrix} \langle -W_1,E^i\rangle \\ \langle -W_2,E^i\rangle \\ \\ \langle -W_M,E^i\rangle \end{bmatrix} \quad (4.13)$$

or

$$[Z_g][I] = [E]$$

The matrix in equation 4.13 is called the generalized impe-
dance matrix; its elements are generalized impedances (6:84).
The remainder of this chapter contains special techniques for
constructing and solving equation 4.13 specifically for the
planar equiangular spiral structure.

   Antenna Symmetry. As shown in Appendix B, the number of
modes needed to represent the open circuited spiral structure
is 4N where N is the number of modes per arm. The generalized
impedance matrix contains an element for every combination of
expansion and test modes. Therefore, since the number of test

31

modes equals the number of expansion modes, there are $(4N)^2$ elements in the matrix. By making use of the antenna symmetry, however, one can reduce the number of unique elements to $4(N)^2$. While the generalized impedance matrix can be arranged arbitrarily, i.e., the modes can be numbered arbitrarily, consider the matrix shown in Figure 4.1. There the matrix is ordered and partitioned to emphasize the arm to arm impedances. Submatrix A_{ij} contains the N^2 generalized impedances between the test modes on the i_{th} arm and the expansion modes on the j_{th} arm. Because of the rotational symmetry of the antenna, the submatrices on the same diagonal are equal. Thus there are $4(N)^2$ unique elements.

Matrix Symmetry. If the test modes are identical to the expansion modes in both functional form and location, then

$$\langle \overline{W}_i, L(\overline{J}_j) \rangle = \langle \overline{J}_i, L(\overline{W}_j) \rangle \tag{4.14}$$

and since reaction is reciprocal,

$$\langle \overline{J}_i, L(\overline{W}_j) \rangle = \langle \overline{W}_j, L(\overline{J}_i) \rangle \tag{4.15}$$

from which it follows that

$$\langle \overline{W}_i, L(\overline{J}_j) \rangle = \langle \overline{W}_j, L(\overline{J}_i) \rangle \tag{4.16}$$

For a matrix with no special properties, symmetry obviously implies that the number of unique elements in the generalized impedance matrix is half that of a matrix without symmetry. For the matrix represented in Figure 4.1 however, the

32

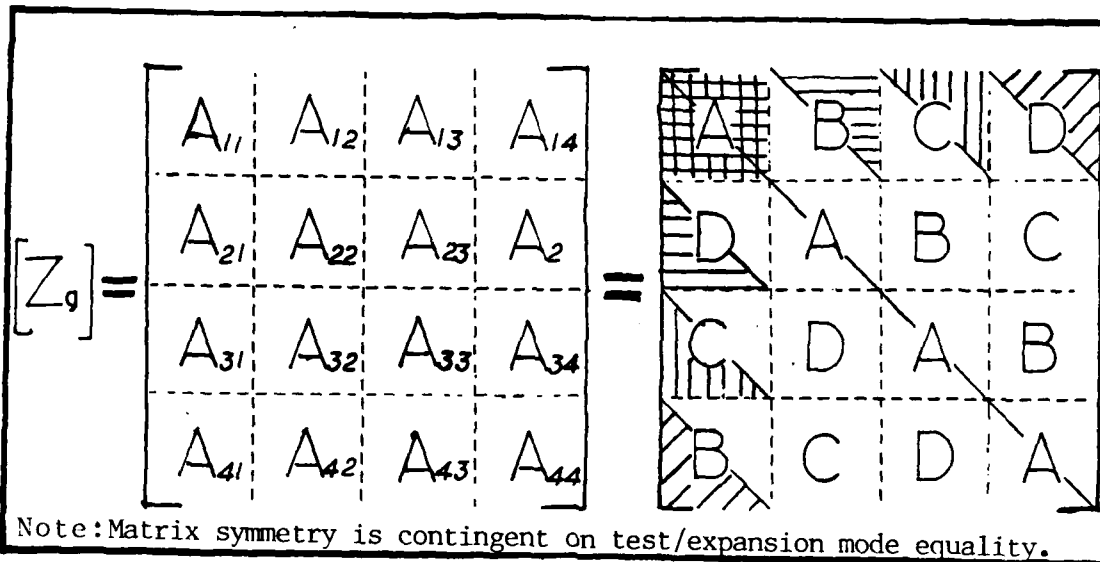Note: Matrix symmetry is contingent on test/expansion mode equality.

Figure 4.1. Generalized Impedance Matrix Showing Effect of Antenna Symmetry (by partitioning) and Matrix Symmetry (by shading).

effect of symmetry is not obvious since the rotational symmetry of the antenna has eliminated the need to compute any element below the diagonal -- except for submatrix A_{11}. Though not obvious, matrix symmetry does further reduce the number of unique elements by a factor of two. The explanation is aided by Figure 4.1, where one can confirm that the elements of the submatraces [A], [B], [C], and [D] obey the following equalities:

$$a_{ij} = a_{ji}$$
$$b_{ij} = d_{ji}$$
$$c_{ij} = c_{ji}$$
$$d_{ij} = b_{ji}$$

Thus if the upper right triangle of each submatrix is computed, the lower left triangles are obtained from the above set of equalities. Although the number of unique elements is decreased

33

by choosing the test modes to be the same as the expansion modes, the computation time for each unique element may increase and outweigh any advantages offered by the symmetric matrix. As explained in Appendix B, the moment method computer code used as a reference (12) represents the modes by filaments of current. The reaction, the generalized impedance, between two modes is the weighted sum of the reactions among the individual filaments. If the expansion modes are represented by K filaments and the test modes are identical to the expansion modes, then there are K^2 filament to filament reactions that require computation for each unique matrix element. If, however, the test modes are represented by a single filament, then there are only K reactions to compute for each unique matrix element. So, while choosing the test modes to be identical with the expansion modes will decrease the matrix computation time by a factor of two by virtue of reciprocity and symmetry, it will increase the time by a factor of K by virtue of the number of test mode filaments. The net increase, then, of time is a factor of K/2 over the single filament test mode case.

Terminal Short Circuits. Chapter 3 explained the need for the computation of the scattered field with the feed network configured as a short circuit between various combinations of two terminals. The model for a short circuit between terminals is explained in Appendix B. The modeling technique requires the addition of one mode for each short. The generalized

34

impedance matrix will be altered by the addition of a row
and a column containing the reactions between the shorting
mode and the modes of the open circuited antenna plus one
element for the mode's self reaction. The generalized
impedance matrix for the short circuited antenna is shown
in Figure 4.2. Assuming that the matrix equation,
$[Z_g][I]=[E_1]$, for the open circuited antenna was solved, the
new equation can be solved with relatively few additional
calculations. Let

$$[I_0] = [Z_g]^{-1}[E_1] \qquad (4.17)$$

represent the solution to the open circuited antenna scat-
tering problem, where $[Z_g]^{-1}[E_1]$ is symbolic of the solution,
regardless of the method used to obtain it. If a new row
and column are added along with an additional unknown, I_2,
and an element, E_2, in the right hand side vector, then the
new system is as shown in Figure 4.2. The corresponding
equations are

$$[Z_g][I_1] + [B]I_2 = [E_1] \qquad (4.18a)$$

$$[C][I_1] + DI_2 = E_2 \qquad (4.18b)$$

Solving for I_2 and $[I_1]$ yields

$$I_2 = \frac{E_2 - [C][I_1]}{D} \qquad (4.19)$$

and

$$[I_1] = [Z_g]^{-1}[E_1] - [Z_g]^{-1}[B]I_2 \qquad (4.20)$$

35
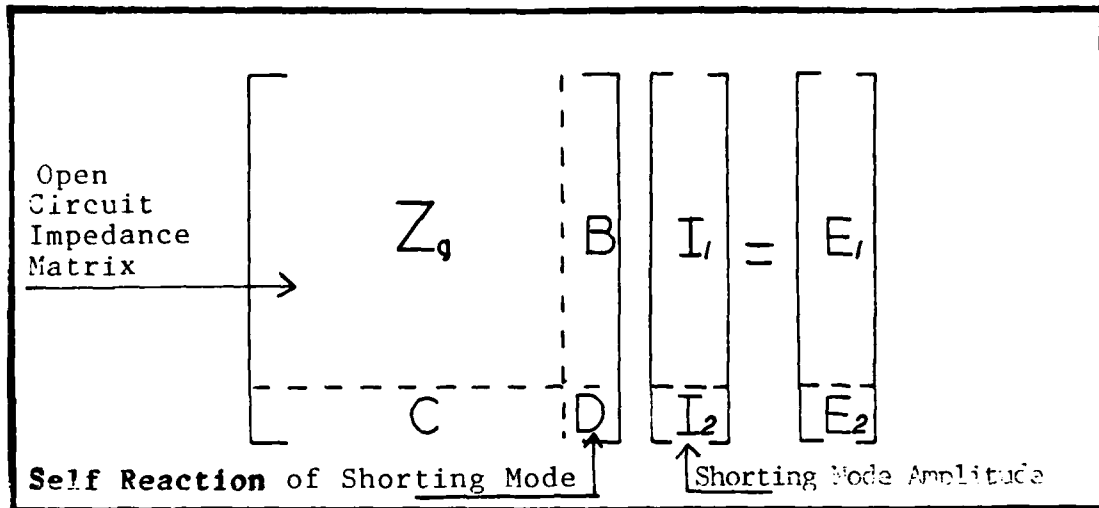
Figure 4.2. Generalized Impedance Matrix of Spiral Antenna with one Shorting Mode.

Applying equation 4.17 to equation 4.20, substituting into equation 4.19 and solving again for I_2 yields

$$I_2 = \frac{E_2 - [C][I_0]}{D - [C][Z_g]^{-1}[B]} \qquad (4.21)$$

and substituting into equation 4.20:

$$[I_1] = [I_0] - [Z_g]^{-1}[B] \frac{E_2 - [C][I_0]}{D - [C][Z_g]^{-1}[B]} \qquad (4.22)$$

If the solution to the "short circuit" equation is obtained without use of equations 4.21 and 4.22, the total number of numerical computer operations is, assuming LU decomposition and M modes, approximately $1/3\ M^3$ (1:152-160). Making use of equations 4.21 and 4.22, one can obtain the "short circuit"

solution with approximately $2M^2$ operations. Note that the evaluation of $[Z_g]^{-1}[B]$ can be made along with other open circuit calculations.

Selection of the Incident Field

Wavelength. The scattering properties of the planar equiangular spiral structure can best be understood if its behavior over a range of wavelengths is known. By making use of the special geometry of the planar equiangular spiral one can avoid the need to recompute the entire generalized impedance matrix of equation 4.13 at each different wavelength. The structure shown in Figure 2.1 represents an antenna with a 6 to 1 wavelength of operation range. Modeling of this structure through the use of equation 3.33 must be done within this range since the assumptions about frequency independent input impedances are not valid outside this range. Also, one must insure that the sizes of the monopole patches are no greater than one fourth wavelength (See Appendix B). Within this band of wavelengths, then, the following explanation is valid.

For the purpose of explanation, the modes of the open circuit spiral structure are grouped into sections, each section comprised of the dipole modes on each arm correspond-ing to the same radial distance. For instance, the innermost four modes -- one on each arm -- are in section 1. The next four modes farther out along the arms form section 2, and so on. (This assumes that only the current modes in the direction
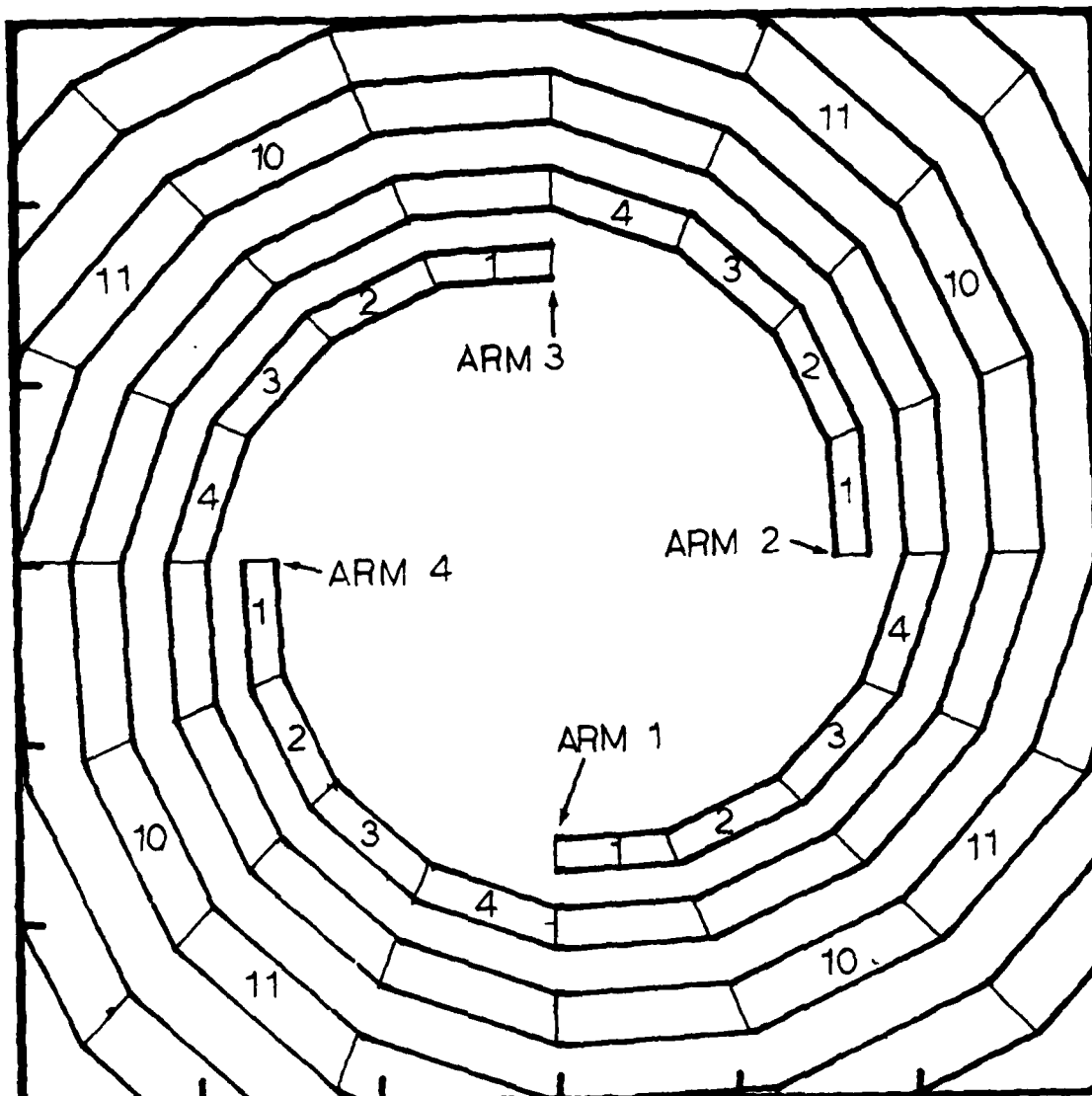
37

Figure 4.3. Patch Representation of Spiral Showing Assignment of Patches into Sections for Purpose of Illustrating the Scaling of the Generalized Impedance Elements.

of the spiral are of interest. If a transverse component
is also modeled, then each section will contain an additional
four modes.) Figure 4.3 illustrates the assignment of modes
into sections. Although two surface patches are associated
with each dipole, the section number is placed in the patch
in which the dipole begins. With this sectioning of modes
the generalized impedance matrix can be partitioned:

$$\left[Z_g\right] = \begin{bmatrix} A_{11} & A_{12} & \bullet\bullet\bullet\bullet & A_{1N} \\ A_{21} & A_{22} & & \\ \bullet & & & \\ \bullet & & & \\ \bullet & & & \\ A_{N1} & & \bullet\bullet\bullet\bullet & A_{NN} \end{bmatrix} \tag{4.23}$$

where A_{ij} is the block of generalized impedances between the
modes in section i and section j:

$$A_{ij}(\lambda) = \begin{bmatrix} Z_{ij}^{11}(\lambda) & Z_{ij}^{12}(\lambda) & Z_{ij}^{13}(\lambda) & Z_{ij}^{14}(\lambda) \\ Z_{ij}^{21}(\lambda) & Z_{ij}^{22}(\lambda) & & \bullet \\ Z_{ij}^{31}(\lambda) & & & \bullet \\ Z_{ij}^{41}(\lambda) & \bullet\ \bullet\ \bullet\ \bullet\ \bullet\ \bullet & & Z_{ij}^{44}(\lambda) \end{bmatrix} \tag{4.24}$$

where the superscripts of Z refer to the arm number as shown
in Figure 4.3. The argument λ emphasizes that the generalized
impedances are computed for a specific wavelength of incident
radiation. The impedance entries in equation 4.24 are sums
of dipole filament to dipole filament impedances, each of
which is a sum of monopole filament to monopole filament
impedances (20:13). A closed form expression exists for
each such impedance (14). The exact expression is not of

39

interest here but its form is. In a lossless medium, the
generalized impedance between two monopoles can be expressed
as a function of two types of arguments:

$$Z = Z(\frac{\overline{\ell}}{\lambda}, \psi) \qquad (4.25)$$

both of which describe the geometry of the two monopoles.
$\overline{\ell}$ is symbolic for several variables all of which are linear
measures, and ψ is the angle between the two monopoles
(See Figure C.1.) Now for any x,

$$Z(\frac{\overline{\ell}}{\lambda_1}, \psi) = Z(\frac{x\,\overline{\ell}}{x\lambda_1}, \psi) \qquad (4.26)$$

That is, the generalized impedance of two monopoles at some
λ_1 is equal to the generalized impedance of two monopoles
scaled by x at a wavelength $x\lambda_1$, assuming ψ remains constant.
Appendix C contains the details of the proof that the geometric
relationship between two monopoles is simply a scaled version
of the relationship between the adjacent set of monopoles.
The scaling factor, K, for adjacent sets of monopoles is a
function of the angular increment, Δ, between adjacent monopoles:

$$K = \exp(\alpha\Delta) \qquad (4.27)$$

where α is defined in equation 2.2. Thus, noting that the
linear dimensions of the monopoles are implicit in the
subscripts of equation 4.24, the elements of equation 4.24 and
the submatrices of equation 4.23 obey the following equalities:

$$Z_{ij}^{mn}(\lambda_1) = Z_{(i+1)(j+1)}^{mn} (K\lambda_1) \qquad (4.28)$$

and

$$A_{ij}(\lambda_1) = A_{(i+1)(j+1)} (K\lambda_1) \qquad (4.29)$$

The relationship between two generalized impedance matrices for two wavelengths related by a factor K is shown below. If the generalized impedance matrix is

$$\left[Z_g \right](\lambda) = \begin{bmatrix} A & B \\ C & D \end{bmatrix} \qquad (4.30)$$

then

$$\left[Z_g \right](K\lambda) = \begin{bmatrix} P & Q \\ R & A \end{bmatrix} \qquad (4.31)$$

where [A] contains the generalized impedances between (N-1) sections. Thus, given that the matrix of equation 4.30 is known, the matrix of equation 4.31 requires only the additional computation of [P], [Q] and [R].

Polarization. It is known from experimental work (4) that the polarization of a wave radiated from a spiral antenna

is elliptical with an axial ratio ranging from 0 to 1. This fact suggest that the scattering analysis should proceed using two orthogonal elliptically polarized waves as the components of the incident and relected waves. Reinforcing this idea is work by Wang (21) which showed the utility of expressing the scattering properties of a spiral structure in terms of left and right hand circularly polarized waves. In Wang's work, the phase of the scattered field was easily predicted only if the fields were expressed as circularly polarized waves. The moment method computer code that is used as a reference for this thesis (12), however, expresses the field in terms of Θ and Φ components of a spherical coordinate system. If we view the scattering matrix, $[S_L]$, in the Θ, Φ coordinate system as a linear operator, then the scattering matrix, $[S_c]$, in the $(\Theta+j\Phi)$, $(\Theta-j\Phi)$ coordinate system is easily found to be

$$[S_c] = [B]^{-1}[S_L][B] \qquad (4.32)$$

where the columns of [B] are the vectors $(1,j)$ and $(1,-j)$, that is, the new basis vectors (9:332). Therefore the scattering matrix for a circularly polarized wave is

$$\left[S_c\right] = \begin{bmatrix} 1 & 1 \\ j & -j \end{bmatrix}^{-1} \begin{bmatrix} S_{L11} & S_{L12} \\ S_{L21} & S_{L22} \end{bmatrix} \begin{bmatrix} 1 & 1 \\ j & -j \end{bmatrix} \qquad (4.33)$$

where

S_{Lij}=scattering matrix element of equation 3.6 for a linearly polarized (Θ,Φ) wave.

42

CHAPTER 5

Conclusions

Techniques for analyzing the scattering properties of a loaded four arm planar equiangular spiral antenna were presented. The two main results of this thesis are the derivation of the scattering equation for the loaded antenna in Chapter 3 and the development of a technique to make use of the moment method generalized impedance elements at different wavelengths in Chapter 4. Implementing these techniques requires a working knowledge of a moment method code like that of reference 12 and some careful "bookkeeping".

Topic for Further Work

The result of Chapter 4, a technique that makes use of the same generalized impedances at different wavelengths, was developed for a self complementary structure. A possible extension of this work to large planar sections could be developed by dividing a plane section into an equiangular spiral and its complement and then applying the technique.

Appendix A

Derivation of the Scattering Impedance

The objective of this appendix is to derive an expression for ΔZ_r in terms of load impedances, port parameters, and short circuited scattering impedances. The expression will be developed from equation 3.12, repeated here

$$
\begin{bmatrix} \Delta V_r \\ V_0 \\ V_1 \\ V_2 \\ V_3 \end{bmatrix} = \begin{bmatrix} \Delta Z_{rr} & Z_{r0} & Z_{r1} & Z_{r2} & Z_{r3} \\ Z_{0r} & Z_0 & Z_1 & Z_2 & Z_3 \\ Z_{1r} & Z_3 & Z_0 & Z_1 & Z_2 \\ Z_{2r} & Z_2 & Z_3 & Z_0 & Z_1 \\ Z_{3r} & Z_1 & Z_2 & Z_3 & Z_0 \end{bmatrix} \begin{bmatrix} I_r \\ I_0 \\ I_1 \\ I_2 \\ I_3 \end{bmatrix} \qquad (3.12)
$$

Solving for ΔV_r yields

$$
\Delta V_r = \Delta Z_{rr} I_r + Z_{r0} I_0 + Z_{r1} I_1 + Z_{r2} I_2 + Z_{r3} I_3 \qquad (A.1)
$$

and for ΔZ_r, the scattering impedance

$$
\Delta Z_r = \frac{\Delta V_r}{I_r} = \Delta Z_{rr} + \frac{\sum_0^3 Z_{rj} I_j}{I_r} \qquad (A.2)
$$

If, in equation A.1, I_r is set to zero and the other currents I_j are set equal to one another; $I_j = I$, then $\Delta V_r = I \sum_0^3 Z_{ri}$. From equation 2.8, $I_j = I$ implies that all terminal currents are zero. Therefore, ΔV_r, which is a measure of the signal received from the spiral, is zero and

$$
\sum_0^3 Z_{ri} \equiv 0 \qquad (A.3)
$$

44

Referring now to equation A.2, ΔZ_r is a function of I_i and therefore of the load impedances. This functional dependance will be denoted by

$$\Delta Z_r = \Delta Z_r \begin{bmatrix} Z_{L0} \\ Z_{L1} \\ Z_{L2} \\ Z_{L3} \end{bmatrix} \tag{A.4}$$

Let $Z_{Li} = \infty$ for all i. Then all terminal currents are zero and, from equation 2.10, the branch currents $I_i = t$ for all i. From equation A.2 and A.3 then,

$$\Delta Z_{rr} = \Delta Z_r \begin{pmatrix} \infty \\ \infty \\ \infty \\ \infty \end{pmatrix} \tag{A.5}$$

Now let $I_1 = I_2 = I_3 = 0$ in equation A.2. From equation 2.8, terminals 2 and 3 must be open circuited $(Z_{L2} = Z_{L3} = \infty)$. If, in addition to this constraint, $Z_{L0} = Z_{L1} = 0$ then $V_0 = 0$ and from the second line of equation 3.12, $I_0 = -Z_{0r} I_r / Z_0$. Substituting into equation A.2 and solving for Z_{0r}^2 yields

$$Z_{0r}^2 = Z_0 [\Delta Z_r \begin{pmatrix} \infty \\ \infty \\ \infty \\ \infty \end{pmatrix} - \Delta Z_r \begin{pmatrix} 0 \\ 0 \\ \infty \\ \infty \end{pmatrix}] \tag{A.6}$$

In a similar manner, it can be shown that

$$Z_{1r}^2 = Z_0 [\Delta Z_r \begin{pmatrix} \infty \\ \infty \\ \infty \\ \infty \end{pmatrix} - \Delta Z_r \begin{pmatrix} 0 \\ 0 \\ \infty \\ \infty \end{pmatrix}] \tag{A.7}$$

$$Z_{2r}^2 = Z_0 [\Delta Z_r \begin{pmatrix} \infty \\ \infty \\ \infty \\ \infty \end{pmatrix} - \Delta Z_r \begin{pmatrix} \infty \\ 0 \\ 0 \\ \infty \end{pmatrix}] \tag{A.8}$$

$$Z_{3r}^2 = Z_0 [\Delta Z_r \begin{pmatrix} \infty \\ \infty \\ \infty \\ \infty \end{pmatrix} - \Delta Z_r \begin{pmatrix} 0 \\ \infty \\ \infty \\ 0 \end{pmatrix}] \tag{A.9}$$

The load constraints on the branch voltages are
(See Figure 3.4)

$$V_0 = Z_{L0}(I_3 - I_0) + Z_{L1}(I_1 - I_0) \qquad (A.10)$$

$$V_1 = Z_{L1}(I_0 - I_1) + Z_{L2}(I_2 - I_1) \qquad (A.11)$$

$$V_2 = Z_{L2}(I_1 - I_2) + Z_{L3}(I_3 - I_2) \qquad (A.12)$$

$$V_3 = Z_{L3}(I_2 - I_3) + Z_{L0}(I_0 - I_3) \qquad (A.13)$$

Making use of the load conditions, letting $I_3 = 0$ (see equation 2.10), and eliminating the last equation of the system in equation 3.12 (since $V_3 = -(V_0 + V_1 + V_2)$) allows one to express the system as

$$-\begin{bmatrix} Z_{0r} \\ Z_{1r} \\ Z_{2r} \end{bmatrix} I_r = \begin{bmatrix} Z_0 + Z_{L0} + Z_{L1} & Z_1 - Z_{L1} & Z_2 \\ Z_3 - Z_{L1} & Z_0 + Z_{L1} + Z_{L2} & Z_1 - Z_{L2} \\ Z_2 & Z_3 - Z_{L2} & Z_0 + Z_{L2} + Z_{L3} \end{bmatrix} \begin{bmatrix} I_0 \\ I_1 \\ I_2 \end{bmatrix} \qquad (A.14)$$

Solving equation A.14 for [I] and substituting into equation A.2 yields

$$\Delta Z_r \begin{bmatrix} Z_{L0} \\ Z_{L1} \\ Z_{L2} \\ Z_{L3} \end{bmatrix} = \Delta Z_r \begin{pmatrix} x \\ x \\ x \end{pmatrix} - \frac{Z_{r0}[Z_{0r}A_{11} + Z_{1r}A_{21} + Z_{2r}A_{31}]}{\Delta}$$

$$- \frac{Z_{r1}[Z_{0r}A_{12} + Z_{1r}A_{22} + Z_{2r}A_{32}]}{\Delta} \qquad (A.15)$$

$$- \frac{Z_{r2}[Z_{0r}A_{13} + Z_{1r}A_{23} + Z_{2r}A_{33}]}{\Delta}$$

where

A_{ij} is the cofactor of the ijth element of the matrix in equation A.14

Δ is the determinent of the matrix equation A.14

$Z_{ri} = Z_{ir}$

One can now solve for Z_{ir} in terms of $Z_r()$ with open and short circuited loads at the terminals.

$$\Delta Z_r \begin{pmatrix} 0 \\ \infty \\ 0 \\ \infty \end{pmatrix} = \Delta Z_r \begin{pmatrix} \infty \\ \infty \\ \infty \\ \infty \end{pmatrix} - \frac{Z_{0r}^2 + Z_{1r}^2 + 2Z_{0r}Z_{1r}}{2(Z_0 + Z_1)} \qquad (A.16)$$

$$\Delta Z_r \begin{pmatrix} \infty \\ 0 \\ \infty \\ 0 \end{pmatrix} = \Delta Z_r \begin{pmatrix} \infty \\ \infty \\ \infty \\ \infty \end{pmatrix} - \frac{Z_{1r}^2 + Z_{2r}^2 + 2Z_{1r}Z_{2r}}{2(Z_0 + Z_1)} \qquad (A.17)$$

and since $Z_{3r} = -(Z_{0r} + Z_{1r} + Z_{2r})$, equation A.9 becomes

$$\Delta Z_r \begin{pmatrix} 0 \\ \infty \\ \infty \\ 0 \end{pmatrix} = Z_r \begin{pmatrix} \infty \\ \infty \\ \infty \\ \infty \end{pmatrix} - \frac{Z_{0r}^2 + Z_{1r}^2 + Z_{2r}^2 + 2Z_{0r}Z_{2r} + 2Z_{0r}Z_{1r} + 2Z_{1r}Z_{2r}}{Z_0}$$

Substituting equations A.6, A.7, A.8, A.16, A.17, and A.18 into equation A.15 results in the scattering impedance as expressed in equation 3.33.

Appendix B

Surface Patch Modeling

Functional Form

The moment method code used as a reference (12) represents surface current as a sum of piecewise sinusoidal surface monopoles. Two adjacent monopoles form a dipole and, as illustrated in Figure B.1, a reference direction is assigned to the current flow. The moment method provides a solution for the phase and magnitude of each dipole. Figure B.1 shows six rectangular sinusoidal surface monopoles joined together to form three overlapping surface dipoles. By adjusting the magnitude and phase of each dipole, one can model a continuous current. Each dipole is called an expansion mode since the current is "expanded" into a linear combination of these modes. Non-rectangular surface currents are modeled similarly, as shown in Figure B.2 (10). Note that in both Figures B.1 and B.2, the current goes to zero at the ends of the dipoles so that no accumulation of charge needs to be accounted for. Though not shown in the figures, there is generally also a surface current running transverse to that shown in the figures.

Numerical Treatment

If the surface monopoles are exact rectangles then the electromagnetic fields associated with them have closed form, exact expressions (15). Otherwise, the fields are found by
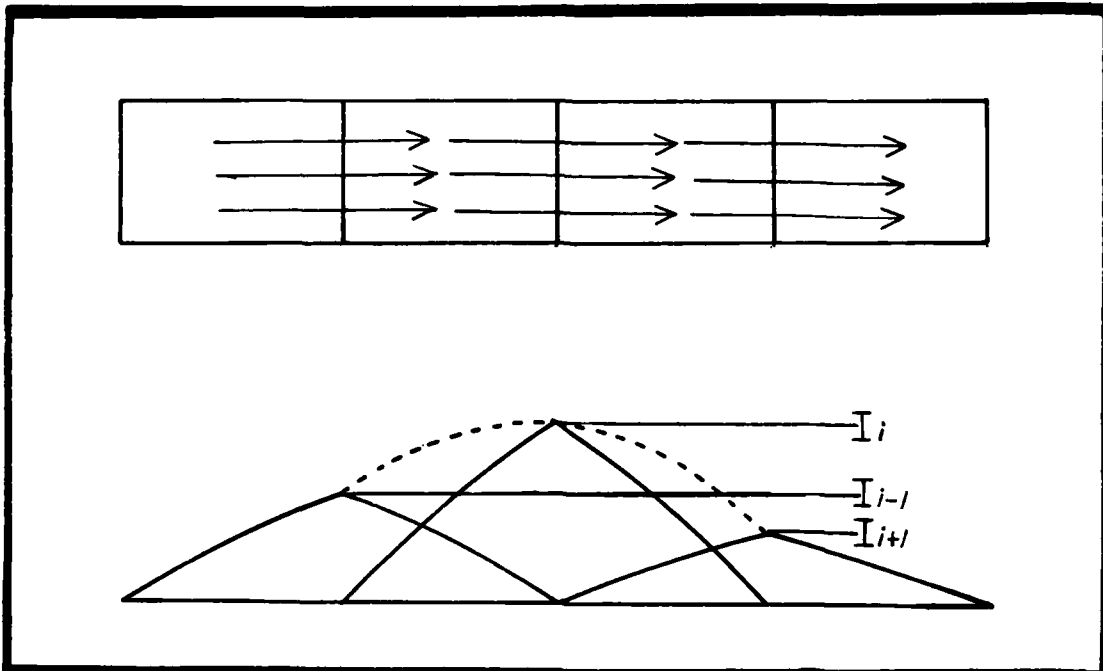
Figure B.1.   Piecewise Continuous Sinusoidal Surface Current
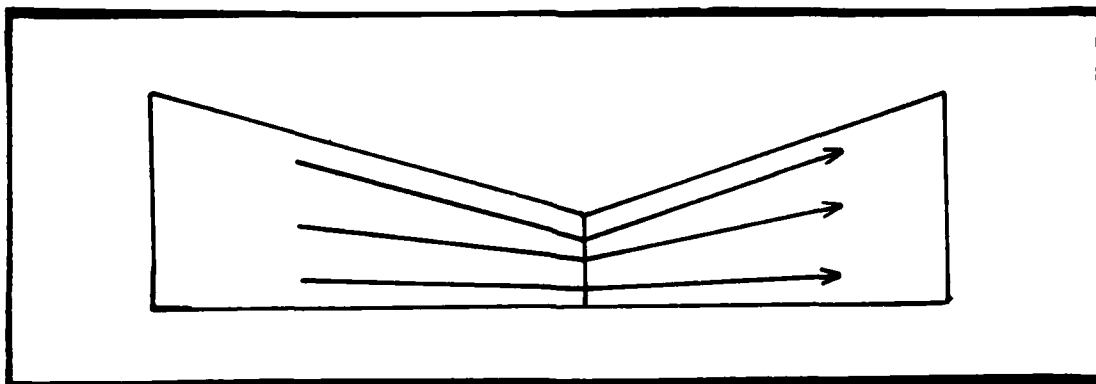on Rectangular Patches.

Source: (12)

Figure B.2.   Non-rectangular Patch Showing Direction of
Surface Current.

Source: (12)

integrating the fields from filamentary sinusoidal monopoles, the fields from five filamentary monopoles are summed (12:27). As expected, the number of integration intervals will affect the field computation time. Work by Tulyathan (20:13) showed that an integration interval of 0.07 times a wavelength is adequate for representing a surface current. Additional precision is obtained only with an increase in computation time. For the antenna structure shown in Figure 2.1, four intervals (five filaments) per segment is sufficient for modeling the component of current in the direction of the spiral. The length of the monopoles also affects both the precision and time of the field calculation. Electromagnetic modeling with monopoles as large as one fourth wavelength yields good results (20:37). The largest patch then on the spiral on which a monopole is superimposed should not exceed one fourth wavelength. For the spiral antenna, the patch length determines the number of monopole patches. The antenna of Figure 2.1 requires N patches per arm or 4N patches total.

Patch Construction

Two methods of subdividing the spiral structure into monopole patches are discussed below.

Skinner constructed the arms of the antenna from quadra-lateral (trapezoidal) patches whose corners are formed by the intersection of radial lines and the spiral curves (19:38). Figure B.3 illustrates this method. Note that the angle between adjacent radials determines the size of each patch.
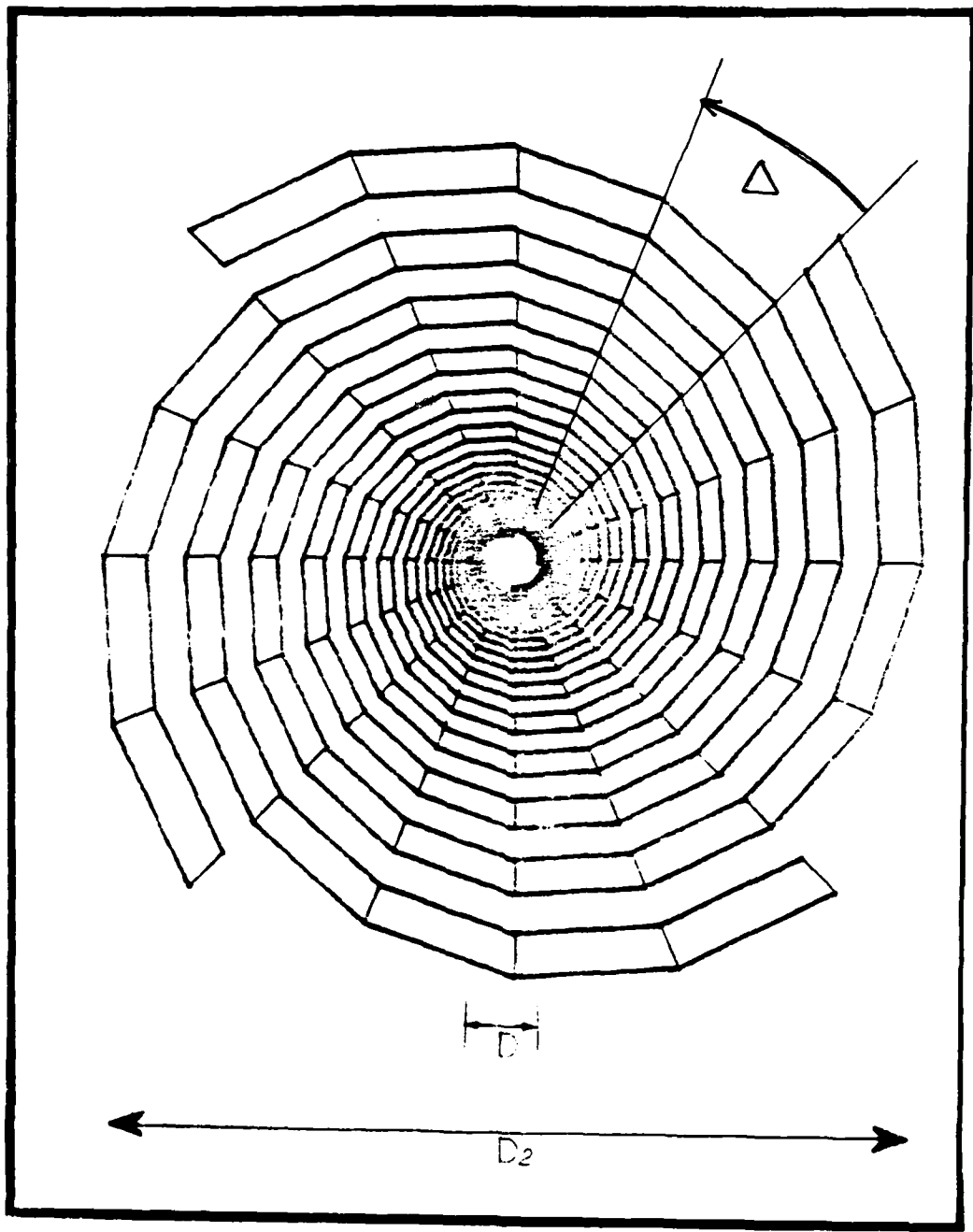
50

Figure B.3. Patch Model of Spiral Antenna.

When the self complementary property of the antenna is to be
modeled, the angle, Δ, must be a submultiple of 45 degrees
so that a rotation of 45 degrees brings the structure back
on its complement. Although division of the arms could be
made at different angular increments (e.g. 45° for the
inner part and 22½° for the outer part) frequency scaling
of the generalized impedance elements as explained in
Chapter 4 is more straightforward if a constant Δ is used.
If Δ =22½°, then the antenna of Figure 2.1 can be modeled
using 204 patches.

Instead of using straight radials to subdivide the
spiral, one can intersect the spiral with a family of
orthogonal curves. The equation of the orthogonal curve
is given by equation B.1

$$\rho = a^{-(\frac{1}{\alpha})^2} \exp[-\frac{1}{\alpha}(\theta - \delta)] \qquad (B.1)$$

where all parameters and variables have the same value
and meaning as in equation 2.2. Note that the orthogonal
curve is also an equiangular spiral but it expands as θ
becomes more negative.

Test Modes

As explained in Chapter 4, the testing functions can
also be thought of as surface currents in a reaction with
the expansion mode currents. For these testing mode currents,
one can choose the same or a different number of filamentary
monopoles to represent the testing modes as is used to

52

represent the expansion modes. Regardless of the number, the functional form of the testing currents in the reference moment method code (12:21) is a piecewise continuous sinusoid.

Terminal Shorting Modes

So far, explanation of the expansion and testing modes has been limited to those modes associated with the open circuited model of the antenna. An additional mode is created by placing a monopole on one arm at the terminal end of the spiral and another monopole on the other arm as illustrated in Figure B.4. The two monopoles together form a single dipole mode whose magnitude and phase can be solved for as explained in Chapter 4. This technique simply provides for the continuity of current from one arm to another.
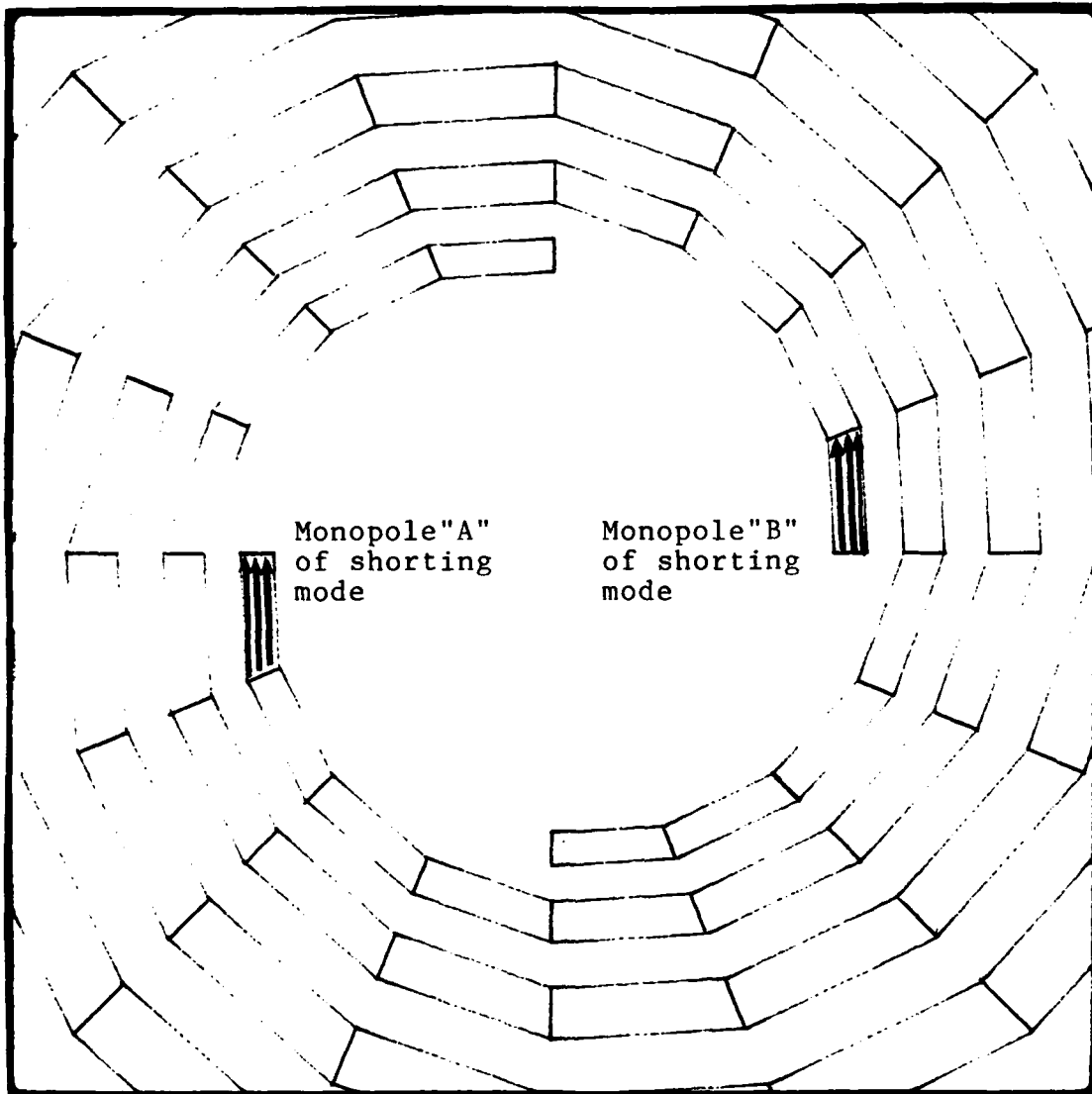
Figure B.4. Terminal Ends of the Spiral Showing the
Construction of a Shorting Mode. Distance
between Monopoles must be Small.

Appendix C

Equiangular Geometry

The purpose of this appendix is to show the relation-ship between the geometry of two adjacent sets of monopoles on an equiangular spiral. This will be done on a filament to filament basis. Reference 14 provides an expression for the mutual impedance between sinusoidal filamentary monopoles. The expression is a function of the geometric parameters shown in Figure C.1: z_1, z_2, t_1, t_2 and Ψ. Although reference 14 pertains to the general three dimen-sional case, only the planar case is pertinent here.
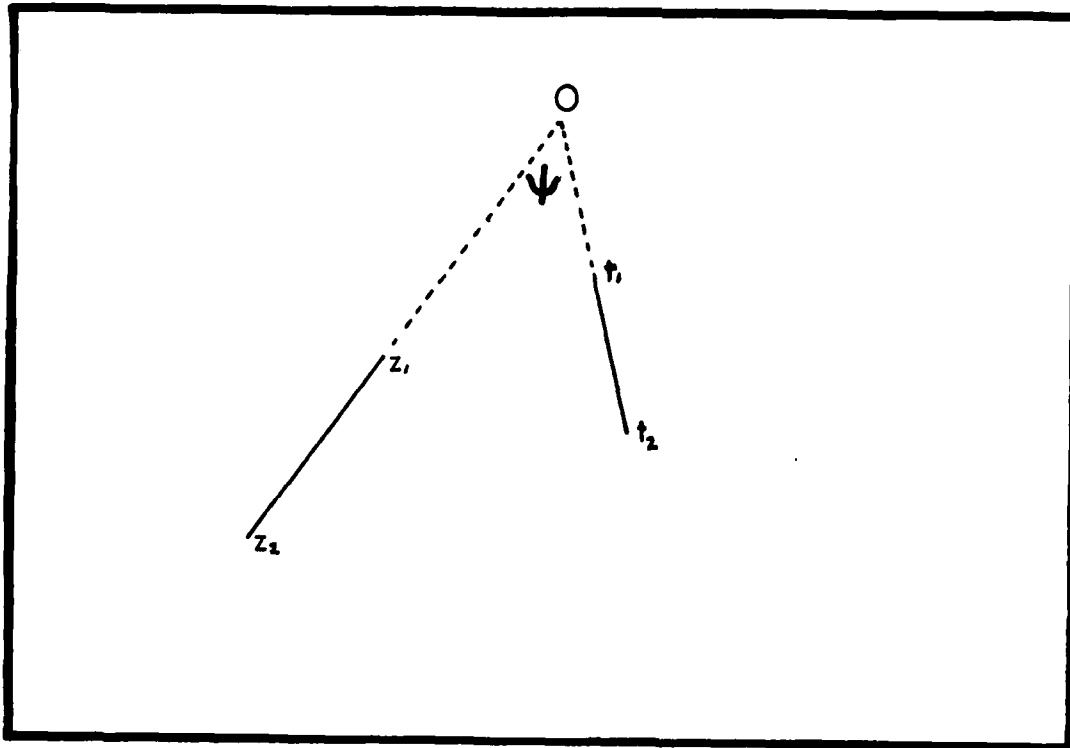

Figure C.1. Filamentary Monopoles with Pertinent Geometric Parameters Shown.
Source: (14)

Figure C.2 shows two monopoles, I and J, and the adjacent set, I+1 and J+1, along with the lengths and angle corresponding to those in Figure C.1. To support the text in Chapter 4, it is sufficient to show that triangles $A_1O_1B_2$ and $B_1O_2A_2$ are similar triangles and that the sides of $A_1O_1B_2$ are K times the sides of $B_1O_2A_2$ where K is from equation 4.27. The similar triangles A_2PB_2, B_2PC_2, C_1PB_1, and B_1PA_1 imply that $\theta_1=\theta_2$. Therefore $\Psi_1=\Psi_2$. Similar triangles A_2PB_1 and B_2PA_1 imply that angle PA_2B_1 equals angle PB_2A_1 and that angle $A_1B_2C_2$ equals angle $B_1A_2B_2$. Therefore, triangles $A_1O_1B_2$ and $B_1O_2A_2$ are similar. And since, by the equiangular construction (equation 2.2), $\overline{PB_2}=K\overline{PA_2}$, then the equality $\overline{A_1B_2}=K\overline{B_1A_2}$ is obtained. Thus the scale factor of the two similar triangles $A_1O_1B_2$ and $B_1O_2A_2$ is K.
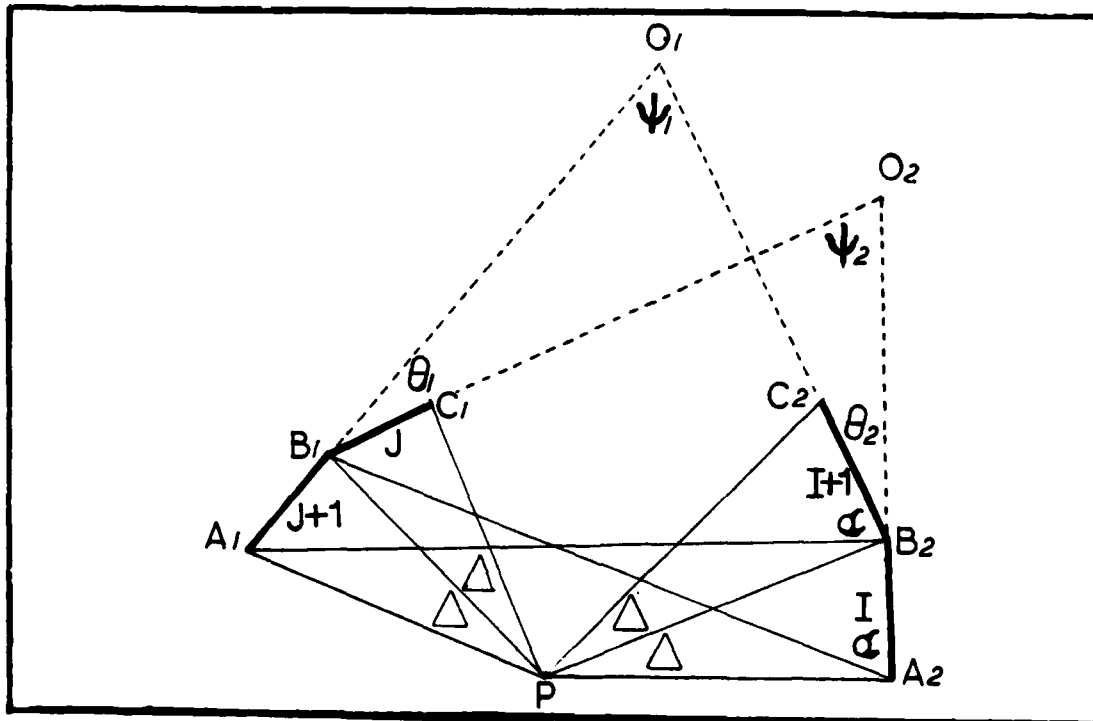

Figure C.2.   Adjacent Sets of Monopoles and Associated Geometry.

Bibliography

1. Björck, Ake and Germund Dahlquist. _Numerical Methods_, translated by Ned Anderson. New Jersey: Prentice-Hall, Inc., 1974.

2. Deschamps, Georges A. "Impedance Properties of Complementary Multiterminal Planar Structures," _IRE Transactions on Antennas and Propagation_, AP-7: S371-S378 (December 1959).

3. Dicke, R. H. and C. G. Montgomery. "Radiation and Scattering By Antennas," _Principles of Microwave Circuits_, edited by C. G. Montgomery. New York: McGraw Hill Book Company, 1948.

4. Dyson, John D. "The Equiangular Spiral Antenna," _IRE Transactions on Antennas and Propagation_, AP-7: 181-187 (April 1959).

5. Green, R. B. _The General Theory of Antenna Scattering_. Report AF 33(616)-8039. Ohio: Antenna Laboratory, 1963.

6. Harrington, Roger F. _Field Computation By Moment Methods_. Florida: Robert E. Krieger Publishing Company, 1983.

7. -----. "Small Resonant Scatterers and Their Use for Field Measurements," _IRE Transactions on Microwave Theory and Techniques_, MTT-10: 165-175 (May 1962).

8. -----. "Theory of Loaded Scatterers," _IEE Proceedings_, 3: 617-623 (April 1964).

9. Mosko, Joseph A. "An Introduction to Wideband Two-Channel Direction-Finding Systems," _Microwave Journal_, 27: 91-106 (February 1984).

10. Newman, Edward H. and Pravit Tulyathan. "A Surface Patch Model for Polygonal Plates," _IEEE Transactions on Antennas and Propagation_, AP-30: 588-593 (July 1982).

11. Newman, E. H. and D. M. Pozar. "Electromagnetic Modeling of Composite Wire and Surface Geometries," _IEEE Transactions on Antennas and Propagation_, AP-26: 784-789 (November 1978).

12. Newman, Edward H. _A User's Manual for Electromagnetic Surface Patch (ESP) Code: Version II - Polygonal Plates and Wires_. Technical Report 717067-4 Contract No. N00014-78-C-0049. Ohio: ElectroScience Laboratory, 1985.

13. Otto, D. V. and J. H. Richmond. "Rigorous Field Expressions for Piecewise-Sinusoidal Line Surfaces," _IEEE Transactions on Antennas and Propagation_, AP-17: 98 (January 1969).

14. Richmond, Jack H. and N. Hugh Geary. "Mutual Impedance of Nonplanar-Skew Sinusoidal Dipoles," _IEEE Transactions on Antennas and Propagation_, AP-23: 412-414 (May 1975).

15. Richmond, Jack H. and D. M. Pozar. "Rigorous Near-Zone Field Expressions for Rectangular Sinusoidal Surface Monopole," _IEEE Transactions on Antennas and Propagation_, AP-26: 509-510 (May 1978).

16. Rumsey, V. H. "Reaction Concept in Electromagnetic Theory," _Physical Review_, 94: 1483-1491 (June 1954).

17. -----. _Frequency Independent Antennas_. New York: Academic Press, 1966.

18. Schelkunoff, Sergei A. and Harold T. Friis. _Antennas, Theory and Practice_. New York: Chapman & Hall, Limited, 1952.

19. Skinner, Second Lieutenant John Paul. _Radiation and Scattering of Spiral Antenna_. MS Thesis, AFIT/GE/ENG/ 184D-60. School of Engineering, Air Force Institute of Technology, Wright-Patterson AFB, OH, _December 1984_.

20. Tulyathan, Pravit. _Moment Method Solutions for Radiation and Scattering from Arbitrarily Shaped Surfaces_. PhD Dissertation. Ohio State University, Columbus, OH, 1981 (8115163).

21. Wang, Johnson J. H. "Characteristics of a New Class of Diode-Switched Integrated Antenna Phase Shifter," _IEEE Transactions on Antennas and Propagation_, AP-31: 156-159 (January 1983).

22. Wang, Nan N. etal. "Sinusoidal Reaction Formulation for Radiation and Scattering from Conducting Surfaces," _IEEE Transactions on Antennas and Propagation_, AP-23: 376-382 (May 1975).

23. Wilton, D. R. etal. "Electromagnetic Scattering By Surfaces of Arbitrary Shape," _Lectures on Computational Methods in Electromagnetics_, edited by Roger F. Harrington etal. Florida: The Scee Press, 1981.

Captain Stephen C. Moraites ███████████████████████
████████████████████████████ He attended high school in
████████████████████████████ he enlisted in the USAF in
1972. He attended the University of Illinois at Urbana
through the AECP program. He graduated from the University
of Illinois in 1981 with high honors and received the degree
of Bachelor of Science in Electrical Engineering. He was
commissioned in the USAF and worked in the field of electro-
magnetic compatibility until entering the School of Engineer-
ing, Air Force Institute of Technology, in May 1984.

REPORT DOCUMENTATION PAGE

1a. REPORT SECURITY CLASSIFICATION	1b. RESTRICTIVE MARKINGS
UNCLASSIFIED	

2a. SECURITY CLASSIFICATION AUTHORITY	3. DISTRIBUTION/AVAILABILITY OF REPORT
	Approved for Public Release;
2b. DECLASSIFICATION/DOWNGRADING SCHEDULE	distribution ulimited

4. PERFORMING ORGANIZATION REPORT NUMBER(S)	5. MONITORING ORGANIZATION REPORT NUMBER(S)
AFIT/GE/ENG/85D-27	

6a. NAME OF PERFORMING ORGANIZATION	6b. OFFICE SYMBOL (If applicable)	7a. NAME OF MONITORING ORGANIZATION

6c. ADDRESS (City, State and ZIP Code)	7b. ADDRESS (City, State and ZIP Code)

8a. NAME OF FUNDING/SPONSORING ORGANIZATION	8b. OFFICE SYMBOL (If applicable)	9. PROCUREMENT INSTRUMENT IDENTIFICATION NUMBER
AFWAL	AAWP-3	

8c. ADDRESS (City, State and ZIP Code)	10. SOURCE OF FUNDING NOS.			
	PROGRAM ELEMENT NO.	PROJECT NO.	TASK NO.	WORK UNIT NO.
Wright-Patterson AFB, OH 45433				

11. TITLE (Include Security Classification)
See box 19

12. PERSONAL AUTHOR(S)
Stephen C. Moraites Capt. USAF

13a. TYPE OF REPORT	13b. TIME COVERED		14. DATE OF REPORT (Yr., Mo., Day)	15. PAGE COUNT
MS Thesis	FROM _____	TO _____	1985 December	66

16. SUPPLEMENTARY NOTATION

17.	COSATI CODES		18. SUBJECT TERMS (Continue on reverse if necessary and identify by block number)
FIELD	GROUP	SUB. GR.	Spiral Antennas, Moment Method
17	03		Loaded Scatterers

19. ABSTRACT (Continue on reverse if necessary and identify by block number)

Title: SCATTERING FROM A PLANAR EQUIANGULAR SPIRAL ANTENNA

Thesis Chairman: Andrew J. Terzuoli, GM-13, DAF

Approved for public release: IAW AFR 190-1/.

(signature) 16 JAN 86
LYN E. WOLAVER
Dean for Research and Professional Development
Air Force Institute of Technology (ATC)
Wright-Patterson AFB OH 45433

20. DISTRIBUTION/AVAILABILITY OF ABSTRACT	21. ABSTRACT SECURITY CLASSIFICATION
UNCLASSIFIED/UNLIMITED ☒ SAME AS RPT. ☐ DTIC USERS ☐	UNCLASSIFIED

22a. NAME OF RESPONSIBLE INDIVIDUAL	22b. TELEPHONE NUMBER (Include Area Code)	22c. OFFICE SYMBOL
Andrew J. Terzuoli GM-13 DAF		AFIT/ENG

DD FORM 1473, 83 APR   EDITION OF 1 JAN 73 IS OBSOLETE.

This thesis presents analytical and numerical techniques for analyzing the scattering from a planar equiangular spiral antenna loaded at its terminals. The scattering matrix for the loaded antenna is derived as a function of the antenna load impedance. This derivation is the result of an analytical study of the voltage/current relationship at the antenna terminals along with an application of a multiport analysis of the scattering problem. A numerical technique is also developed that utilizes at different wavelengths common elements of the generalized impedance matrix of the moment method solution. This technique provides for rapid computation of the scattering properties of the spiral antenna across a band of frequencies.